General formulations for computing the optical gradient and scattering forces on a spherical chiral particle immersed in generic monochromatic optical fields

Hongxia Zheng,[1,2] Xiao Li,[3] Yikun Jiang,[4] Jack Ng,[5] Zhifang Lin,[1,6,*] and Huajin Chen[1,2,†]

[1]*State Key Laboratory of Surface Physics, Key Laboratory of Micro- and Nanophotonic Structures and Department of Physics, Fudan University, Shanghai 200433, China*

[2]*School of Electrical and Information Engineering, Guangxi University of Science and Technology, Liuzhou, Guangxi 545006, China*

[3]*Department of Physics, The Hong Kong University of Science and Technology, Hong Kong, China*

[4]*Department of Physics, Cornell University, Ithaca, New York 14853, USA*

[5]*Department of Physics, Southern University of Science and Technology, Shenzhen 518055, China*

[6]*Collaborative Innovation Center of Advanced Microstructures, Nanjing University, Nanjing 210093, China*

(Received 26 February 2020; accepted 21 April 2020; published 14 May 2020)

We present the Cartesian multipole expansion theory for computing the optical force acting on a spherical chiral particle immersed in generic monochromatic optical fields. The theory enables us to develop the general formulations for individually calculating the optical gradient and scattering forces (also known as the conservative and nonconservative forces) on a spherical chiral particle of arbitrary size. A set of analytical expressions are then derived for the gradient and scattering forces acting on a chiral particle in arbitrary optical field modeled by a series of homogenous plane waves. As examples of applications, we reveal that, in optical lattice composed of three interferential plane waves, the profiles of the in-plane optical gradient and scattering force acting on a spherical chiral particle show higher degree of symmetry and exhibit invariance with respect to the particle size, material composition, and chirality. The remarkable characteristics are totally masked in the undecomposed optical total force. The rigorous analytical decomposition of optical force sheds some more light on the physical understanding of light-matter interaction, it may also contribute significantly to the design of optical beams for achieving more diversified optical micromanipulation on chiral particles.

DOI: 10.1103/PhysRevA.101.053830

I. INTRODUCTION

Chirality, widespread in nature at a variety of size scales, describes the geometrical property of structures which are nonsuperimposable with their mirror images no matter how you rotate and translate them [1]. The human hand is a typical example. The detection and separation of substance by its chirality has developed into a vibrant research field, especially in the pharmaceutical industry, since the function of biomedicine is strongly related to a molecule's chirality. A cure can become poison if its chirality is reversed [2]. For instance, a chiral biomolecule with inverted chirality will turn inactive or toxic to cells, which may result in many diseases such as Alzheimer's, Parkinson's, and type II diabetes [3]. In recent years, chiral separation with the help of optomechanics has attracted broad interest [4–10] because it is, as a contactless tool, less invasive and more efficient compared with other chemical methods [11].

The principle of optomechanics lies in the mechanical effect of light [12–14]. Light carries linear momentum, which can be transferred to particle on its propagating way, pushing the latter along the light propagation direction, known as radiation force in an intuitive sense. Kepler was the first to be aware of this mechanical effect of light, for example, by considering that the tail of a comet pointing away from the sun was caused by the sun's radiation pressure [15]. The first scientific evolution in the application of optical force, attributed to the advent of the laser, was put forward over 350 years later by Ashkin, who successfully implemented the optical acceleration and trapping of a micron-sized particle, taking advantage of the radiation scattering force in 1970 [16]. Later, he and his collaborators experimentally trapped a dielectric particle using a single highly focused Gaussian laser beam, which develops into the concept of optical tweezers [17]. The optical tweezers technology, marking a milestone in the history of the practical applications of optical force, is also a breakthrough of paramount importance in the understanding of light-matter interaction, since scientists begin to recognize the existence of gradient force originating from the inhomogeneity of optical field, which does not necessarily point along the direction of light propagation in general, dramatically distinct from the early known radiation pressure, or, say, scattering force.

Optical gradient force and scattering force, or, in a more physical sense, conservative force and nonconservative force, are two essentially different parts constituting the optical force. They play rather different roles in the optical manipulation. In general, the conservative gradient force is usually responsible for optical trapping and a scalar optical potential energy can be defined [12,17–19], while the nonconservative scattering force [20] can propel [16,19–23] or pull [24–28]

*phlin@fudan.edu.cn

†huajinchen13@fudan.edu.cn

objects, achieving particle transportation, even along curved trajectories [22,23]. Separately calculating the gradient and scattering parts of the optical force is therefore desirable for the design of various optical manipulations based on their obvious different properties as well as for the understanding of light-matter interaction. However, the decomposition has not been successful for a long time, except in two limiting cases where particle is either much smaller (dipole approximation) [29] or much larger (ray-optics approximation) [30] than operating optical wavelength, due to complex mathematics. The partition of the optical force acting on the most experimentally accessible Mie particle remains open for over 30 years since the concepts were demonstrated by Ashkin [17]. It is until recently that Du and coauthors proposed a purely numerical approach on the basis of the Helmholtz decomposition and fast Fourier transform (FFT) [31] and successfully depicted the individual profiles of the gradient force and scattering force acting on the Mie particle. The FFT-based algorithm generally requires numerical computation of optical forces over entire space before performing the separation, imposing a demand for computing facilities and severely limiting the calculation speed, besides obscuring the physical understanding. Very recently, we proposed a semianalytical formulation [32] within the frame of the generalized Lorenz-Mie theory [33], which removes the speed limitation and reduces the facility demand brought by the nonlocal FFT-based decomposition method. Later on, the analytical expressions were derived for the decomposition of optical force on conventional particles through modeling the general optical fields by a set of homogeneous plane waves [34–36], based on the general separation formulations presented before [37,38]. The optical force on a spherical particle in Bessel beams is analytically decomposed into the conservative and nonconservative parts [39].

Unlike the development of the optical force decomposition approaches for conventional isotropic particles, the partition of the optical force exerted on chiral particles has always been elusive, even for the two extreme cases with particle size much larger or smaller than the optical wavelength, due to the forbiddingly complex algebra compared with the case of conventional particles. In this paper, we derive the general formulations for the calculation of optical force as well as its decomposed conservative and nonconservative constituents on the basis of the Cartesian multipole expansion theory [37,38]. With the help of the general formulations, we also develop a set of analytical expressions for both constituent forces due to generic illuminating optical fields modeled by a series of plane waves. As examples of applications, we compute the gradient and scattering forces on a chiral particle immersed in three-wave interference fields (TWIF) [34,36,40]. The hidden symmetry and invariance of the decomposed optical forces, as previously reported for a conventional particle [34], manifest even when particle chirality comes into play.

II. ALGORITHMS DESCRIPTION

In this section, we present the Cartesian multipole expansion theory for the time-averaged optical force $\langle \boldsymbol{F} \rangle$ acting on a chiral spherical particle of arbitrary size and composition immersed in general monochromatic optical fields, followed by the decomposition of the optical force $\langle \boldsymbol{F} \rangle$ into the gradient part $\boldsymbol{F_g} = -\nabla\varphi$ and scattering part $\boldsymbol{F_s} = \nabla \times \boldsymbol{\psi}$, with $\langle \boldsymbol{F} \rangle = \boldsymbol{F_g} + \boldsymbol{F_s}$. Taking advantage of the Cartesian multipole expansion theory, we next derive the rigorous analytical expressions for $\boldsymbol{F_g}$ and $\boldsymbol{F_s}$ acting on a chiral sphere residing in optical field composed of arbitrary number of plane waves with any polarizations and amplitudes. The formulations can thus apply to generic monochromatic illuminating optical fields, since the latter are simply a superposition of plane waves.

A. Optical force by Cartesian multipole expansion theory

To begin with, let us recapitulate the expressions of optical force acting on a generic particle within the Cartesian multipole expansion theory, which have been derived before by Jiang *et al.* [37,38]. Physically, it is convenient to consider light scattering as two processes when evaluating optical force. First, light is intercepted by the particle in the way of its propagation, exerting interception (extinction) force on the particle owing to the optical momentum transfer. Second, light is re-emitted due to the excitation of multipoles on the scatterer, resulting in recoil force that does not have an analog in static case. As a result, the time-averaged optical force acting on arbitrary particle immersed in any monochromatic optical field can be written as a sum of interception (extinction) force $\langle \boldsymbol{F}_{\rm int} \rangle$ and recoil force $\langle \boldsymbol{F}_{\rm rec} \rangle$ [24,37,38,41], with $\langle \cdot \rangle$ denoting the time average. Based on the T-matrix method [42,43], the multipole field theory [44,45], and the irreducible tensor theory [46], both forces, $\langle \boldsymbol{F}_{\rm int} \rangle$ and $\langle \boldsymbol{F}_{\rm rec} \rangle$, can be expressed in terms of the electric and magnetic multipoles of various orders induced on the particle as well as the multiple gradient of electric and magnetic fields impinging on the scatterer. To be specific, they read [37,38]

$$\langle \boldsymbol{F}_{\rm int} \rangle = \sum_{l=1}^{\infty} \langle \boldsymbol{F}_{\rm int}^{(l)} \rangle, \tag{1a}$$

$$\langle \boldsymbol{F}_{\rm int}^{(l)} \rangle = \langle \boldsymbol{F}_{\rm int}^{\rm e(l)} \rangle + \langle \boldsymbol{F}_{\rm int}^{\rm m(l)} \rangle, \tag{1b}$$

$$\langle \boldsymbol{F}_{\rm int}^{\rm e(l)} \rangle = \frac{1}{2\,l!}\,{\rm Re}\big[(\nabla^{(l)}\boldsymbol{E}^*) \overset{(l)}{\cdot\cdot} \overset{\leftrightarrow}{\mathbb{O}}{}^{(l)}_{\rm elec}\big], \tag{1c}$$

$$\langle \boldsymbol{F}_{\rm int}^{\rm m(l)} \rangle = \frac{1}{2\,l!}\,{\rm Re}\big[(\nabla^{(l)}\boldsymbol{B}^*) \overset{(l)}{\cdot\cdot} \overset{\leftrightarrow}{\mathbb{O}}{}^{(l)}_{\rm mag}\big], \tag{1d}$$

and

$$\langle \boldsymbol{F}_{\rm rec} \rangle = \sum_{l=1}^{\infty} \langle \boldsymbol{F}_{\rm rec}^{(l)} \rangle, \tag{2a}$$

$$\langle \boldsymbol{F}_{\rm rec}^{(l)} \rangle = \langle \boldsymbol{F}_{\rm rec}^{\rm e(l)} \rangle + \langle \boldsymbol{F}_{\rm rec}^{\rm m(l)} \rangle + \langle \boldsymbol{F}_{\rm rec}^{\rm x(l)} \rangle, \tag{2b}$$

$$\langle \boldsymbol{F}_{\rm rec}^{\rm e(l)} \rangle = -\frac{1}{4\pi\varepsilon_0} \frac{(l+2)\,2^{l+1}\,k^{2l+3}}{(2l+3)!}\,{\rm Im}\big[\overset{\leftrightarrow}{\mathbb{O}}{}_{\rm elec}^{(l)*} \overset{(l)}{\cdot\cdot} \overset{\leftrightarrow}{\mathbb{O}}{}_{\rm elec}^{(l+1)}\big], \tag{2c}$$

$$\langle \boldsymbol{F}_{\rm rec}^{\rm m(l)} \rangle = -\frac{\mu_0}{4\pi} \frac{(l+2)\,2^{l+1}\,k^{2l+3}}{(2l+3)!}\,{\rm Im}\big[\overset{\leftrightarrow}{\mathbb{O}}{}_{\rm mag}^{(l)*} \overset{(l)}{\cdot\cdot} \overset{\leftrightarrow}{\mathbb{O}}{}_{\rm mag}^{(l+1)}\big], \tag{2d}$$

$$\langle \boldsymbol{F}_{\rm rec}^{\rm x(l)} \rangle = \frac{Z_0}{4\pi} \frac{2^l\,k^{2l+2}}{l\,(2l+1)!}\,{\rm Re}\big[\overset{\leftrightarrow}{\mathbb{O}}{}_{\rm elec}^{(l)} \overset{(l-1)}{\cdot\cdot} \overset{\leftrightarrow}{\mathbb{O}}{}_{\rm mag}^{(l)*}\big] \overset{(2)}{\cdot\cdot} \overset{\leftrightarrow}{\boldsymbol{\epsilon}}, \tag{2e}$$

where the superscript * designates the complex conjugate; k, ε_0, μ_0, and $Z_0 = \sqrt{\mu_0/\varepsilon_0}$ are, respectively, the wave number, permittivity, permeability, and wave impedance in the transparent (lossless) fluid medium in which the particle resides; $\boldsymbol{E}$ and $\boldsymbol{B}$ denote the incident electric and magnetic fields impinging on the particle, respectively; $\overset{\leftrightarrow}{\boldsymbol{\epsilon}}$ is the Levi-Civita tensor, whose components ϵ_{ijk} are antisymmetric with respect to the permutation of any pair of indices; and, finally, the superscripts "e," "m," and "x" denote, respectively, the contributions due to the electric multipoles, magnetic multipoles, and hybrid terms. The multiple contraction between two tensors of ranks l and l', denoted by $\overset{(m)}{\cdot\cdot}$, is given by

$$\overset{\leftrightarrow}{\mathbb{A}}{}^{(l)} \overset{(m)}{\cdot\cdot} \overset{\leftrightarrow}{\mathbb{B}}{}^{(l')} = \mathbb{A}^{(l)}_{i_1\,i_2\,\cdots\,i_{l-m}\,k_1\,k_2\,\cdots\,k_m}\,\mathbb{B}^{(l')}_{k_m\,\cdots\,k_2\,k_1\,j_{m+1}\,j_{m+2}\,\cdots\,j_{l'}}, \qquad 0 \leqslant m \leqslant \min[\,l,l'\,], \tag{3}$$

where the summation over repeated indices is assumed. The totally symmetric and traceless [47] rank-l tensors $\overset{\leftrightarrow}{\mathbb{O}}{}_{\rm elec}^{(l)}$ and $\overset{\leftrightarrow}{\mathbb{O}}{}_{\rm mag}^{(l)}$, usually referred to as 2^l-pole, are derived based on the multipole fields theory [44] and by comparing electromagnetic fields radiated from multipoles $\overset{\leftrightarrow}{\mathbb{O}}{}_{\rm elec}^{(l)}$ and $\overset{\leftrightarrow}{\mathbb{O}}{}_{\rm mag}^{(l)}$ with those written in terms of vector spherical wave functions (see Appendix A). The final results read

$$\overset{\leftrightarrow}{\mathbb{O}}{}_{\rm elec\,(mag)}^{(l)} = \gamma_{\rm e\,(m)}^{(l)} \sum_{m=0}^{\lfloor \frac{l-1}{2} \rfloor} d_{l,m}\,k^{2m}\,\overset{\leftrightarrow}{\mathbb{N}}{}_{\rm elec\,(mag)}^{(l,\,m)} \pm \gamma_{\rm x}^{(l)} \sum_{m=0}^{\lfloor \frac{l-1}{2} \rfloor} d_{l,m}\,k^{2m}\,\overset{\leftrightarrow}{\mathbb{N}}{}_{\rm mag\,(elec)}^{(l,\,m)},$$
$$d_{l,m} = \frac{1}{4^m}\,\frac{l!}{m!}\,\frac{\Gamma\big(l-m+\frac{1}{2}\big)}{\Gamma\big(l+\frac{1}{2}\big)\,\Gamma(l-2m)}\,\frac{1}{l}, \qquad \text{with} \quad d_{l,0} = 1, \tag{4}$$

where the upper and lower signs before $\gamma_{\rm x}^{(l)}$ correspond, respectively, to electric and magnetic multipoles, $\overset{\leftrightarrow}{\mathbb{O}}{}_{\rm elec}^{(l)}$ and $\overset{\leftrightarrow}{\mathbb{O}}{}_{\rm mag}^{(l)}$, whereas $\lfloor x \rfloor$ gives the greatest integer less than or equal to x and $\Gamma(x)$ denotes the Γ function. The lowest order cases with, e.g., $l = 1, 2, 3$, and 4, are known as the dipole moment, quadrupole moment, octupole moment, and hexadecapole moment, respectively. For instance, $\overset{\leftrightarrow}{\mathbb{O}}{}_{\rm elec}^{(1)}$ and $\overset{\leftrightarrow}{\mathbb{O}}{}_{\rm mag}^{(1)}$ reduce to the electric and magnatic dipole moments induced on the chiral spherical particle, $\overset{\leftrightarrow}{\mathbb{O}}{}_{\rm elec}^{(1)} = \boldsymbol{p} = \gamma_{\rm e}^{(1)}\boldsymbol{E} + \gamma_{\rm x}^{(1)}\boldsymbol{B}$ and $\overset{\leftrightarrow}{\mathbb{O}}{}_{\rm mag}^{(1)} = \boldsymbol{m} = \gamma_{\rm m}^{(1)}\boldsymbol{B} - \gamma_{\rm x}^{(1)}\boldsymbol{E}$. The electric and magnetic polarizabilities, $\gamma_{\rm e}^{(l)}$, $\gamma_{\rm m}^{(l)}$, and $\gamma_{\rm x}^{(l)}$, depend on the Mie coefficients [42,48] a_l, b_l, and c_l of a spherical chiral particle through

$$\gamma_{\rm e}^{(l)} = \frac{i\,\zeta_l\,a_l}{k^{2l+1}}, \quad \gamma_{\rm m}^{(l)} = \frac{i\,c^2\zeta_l\,b_l}{k^{2l+1}}, \quad \gamma_{\rm x}^{(l)} = -\frac{c\,\zeta_l\,c_l}{k^{2l+1}}, \quad \text{with} \quad \zeta_l = \frac{4\pi\varepsilon_0 l(2l+1)!!}{(l+1)}, \tag{5}$$

with i denoting an imaginary unit and c being the speed of light in the ambient medium. The multipole moments, as described in Eq. (4), degenerate into the nonchiral conventional spherical particle presented by Jiang *et al.* [38] if one sets $\gamma_{\rm x}^{(l)} = 0$. The totally traceless and symmetric rank-l tensors $\overset{\leftrightarrow}{\mathbb{N}}{}_{\rm elec\,(mag)}^{(l,\,m)}$ are given by

$$\overset{\leftrightarrow}{\mathbb{N}}{}_{\rm elec\,(mag)}^{(l,\,m)} = \hat{\mathcal{S}}\Big[\overbrace{\overset{\leftrightarrow}{\mathbb{I}} \otimes \overset{\leftrightarrow}{\mathbb{I}} \otimes \cdots \overset{\leftrightarrow}{\mathbb{I}} \otimes}^{m}\ \overset{\leftrightarrow}{\mathbb{M}}{}_{\rm elec\,(mag)}^{(l-2m)}\Big] \qquad \text{with} \quad \overset{\leftrightarrow}{\mathbb{N}}{}_{\rm elec\,(mag)}^{(l,\,0)} \equiv \overset{\leftrightarrow}{\mathbb{M}}{}_{\rm elec\,(mag)}^{(l)}, \tag{6}$$

where $\overset{\leftrightarrow}{\mathbb{I}}$ denotes the unit dyad of dimension 3 and $\hat{\mathcal{S}}$ denotes the symmetrizing operator, whereas the symbol $\otimes$ represents the tensor product so that the term in the square brackets means taking tensor product by m consecutive times, resulting in a tensor with rank $l - m$. The tensors $\overset{\leftrightarrow}{\mathbb{M}}{}_{\rm elec\,(mag)}^{(n)}$ are two sets of totally symmetric tensors of rank n describe the symmetrized multiple gradient of incident fields

$$\overset{\leftrightarrow}{\mathbb{M}}^{(n)}_{\text{elec}} = \hat{\mathcal{S}}[\,\nabla^{(n-1)}\boldsymbol{E}\,] = \hat{\mathcal{S}}[\,\overbrace{\nabla\nabla\cdots\nabla}^{n-1}\boldsymbol{E}\,] = \frac{1}{n}\sum_{j=1}^{n}\partial_{i_1}\cdots\partial_{i_{j-1}}\partial_{i_n}\partial_{i_{j+1}}\cdots\partial_{i_{n-1}}E_{i_j},$$

$$\overset{\leftrightarrow}{\mathbb{M}}^{(n)}_{\text{mag}} = \hat{\mathcal{S}}[\,\nabla^{(n-1)}\boldsymbol{B}\,] = \hat{\mathcal{S}}[\,\overbrace{\nabla\nabla\cdots\nabla}^{n-1}\boldsymbol{B}\,] = \frac{1}{n}\sum_{j=1}^{n}\partial_{i_1}\cdots\partial_{i_{j-1}}\partial_{i_n}\partial_{i_{j+1}}\cdots\partial_{i_{n-1}}B_{i_j}, \tag{7}$$

where $\nabla^{(n)}$ means taking n consecutive gradients on a scalar or vector field, E_j (B_j) is the jth Cartesian component of the electric (magnetic) field, and ∂_i represents the partial derivative $\frac{\partial}{\partial x_i}$ with respect to the ith Cartesian coordinate. The tensors $\overset{\leftrightarrow}{\mathbb{M}}^{(n)}_{\text{elec (mag)}}$ so defined are obviously invariant under the permutation of any pair of indices so they are totally symmetric, but they are not totally traceless (vanishing under the contraction of any pair of indices) [47].

B. Optical force and its decomposition for generic incident fields

To separate the optical force exerting on a spherical particle into the conservative and nonconservative parts, viz. an irrotational term of zero curl and a solenoidal term of zero divergence, it is convenient to write the optical force in terms of the multiple gradients $\overset{\leftrightarrow}{\mathbb{M}}^{(n)}_{\text{elec}}$ and $\overset{\leftrightarrow}{\mathbb{M}}^{(n)}_{\text{mag}}$ of the electric and magnetic fields defined in Eq. (7), instead of multipole moments $\overset{\leftrightarrow}{\mathbb{O}}^{(l)}_{\text{elec}}$ and $\overset{\leftrightarrow}{\mathbb{O}}^{(l)}_{\text{mag}}$, so that we can separate the Mie coefficients characterizing the particle property from the impinging fields, facilitating the decomposition. After lengthy algebra, the results read

$$\langle \boldsymbol{F}^{\text{e}(l)}_{\text{int}}\rangle = \frac{1}{2\,l!}\,\text{Re}\sum_{m=0}^{\lfloor\frac{l-1}{2}\rfloor} c_{l,m}k^{4m}\big[\gamma^{(l)}_{\text{e}}\boldsymbol{t}^{(l-2m)}_{\text{ee}} + \gamma^{(l)}_{\text{x}}\boldsymbol{t}^{(l-2m)}_{\text{me}}\big], \tag{8a}$$

$$\langle \boldsymbol{F}^{\text{m}(l)}_{\text{int}}\rangle = \frac{1}{2\,l!}\,\text{Re}\sum_{m=0}^{\lfloor\frac{l-1}{2}\rfloor} c_{l,m}k^{4m}\big[\gamma^{(l)}_{\text{m}}\boldsymbol{t}^{(l-2m)}_{\text{mm}} - \gamma^{(l)}_{\text{x}}\boldsymbol{t}^{(l-2m)}_{\text{em}}\big], \tag{8b}$$

$$\begin{aligned}\langle \boldsymbol{F}^{\text{e}(l)}_{\text{rec}}\rangle = -\frac{k^{2l+5}}{l!\,\zeta_{l+1}}\,\text{Im}\sum_{m=0}^{\lfloor\frac{l-1}{2}\rfloor}\big\{&f_{l,m}k^{4m-2}\big[\eta^{(l)}_{\text{ee}}\boldsymbol{\tau}^{(l-2m)*}_{\text{ee}} + \eta^{(l)}_{\text{ex}}\boldsymbol{\tau}^{(l-2m)*}_{\text{em}} + \eta^{(l)}_{\text{xe}}\boldsymbol{\tau}^{(l-2m)*}_{\text{me}} + \eta^{(l)}_{\text{xx}}\boldsymbol{\tau}^{(l-2m)*}_{\text{mm}}\big]\\ &+g_{l,m}k^{4m}\big[\eta^{(l)}_{\text{ee}}\boldsymbol{\tau}^{(l-2m-1)}_{\text{ee}} + \eta^{(l)}_{\text{ex}}\boldsymbol{\tau}^{(l-2m-1)}_{\text{me}} + \eta^{(l)}_{\text{xe}}\boldsymbol{\tau}^{(l-2m-1)}_{\text{em}} + \eta^{(l)}_{\text{xx}}\boldsymbol{\tau}^{(l-2m-1)}_{\text{mm}}\big]\big\},\end{aligned} \tag{8c}$$

$$\begin{aligned}\langle \boldsymbol{F}^{\text{m}(l)}_{\text{rec}}\rangle = -\frac{k^{2l+5}}{c^2 l!\,\zeta_{l+1}}\,\text{Im}\sum_{m=0}^{\lfloor\frac{l-1}{2}\rfloor}\big\{&f_{l,m}k^{4m-2}\big[\eta^{(l)}_{\text{mm}}\boldsymbol{\tau}^{(l-2m)*}_{\text{mm}} - \eta^{(l)}_{\text{mx}}\boldsymbol{\tau}^{(l-2m)*}_{\text{me}} - \eta^{(l)}_{\text{xm}}\boldsymbol{\tau}^{(l-2m)*}_{\text{em}} + \eta^{(l)}_{\text{xx}}\boldsymbol{\tau}^{(l-2m)*}_{\text{ee}}\big]\\ &+g_{l,m}k^{4m}\big[\eta^{(l)}_{\text{mm}}\boldsymbol{\tau}^{(l-2m-1)}_{\text{mm}} - \eta^{(l)}_{\text{mx}}\boldsymbol{\tau}^{(l-2m-1)}_{\text{em}} - \eta^{(l)}_{\text{xm}}\boldsymbol{\tau}^{(l-2m-1)}_{\text{me}} + \eta^{(l)}_{\text{xx}}\boldsymbol{\tau}^{(l-2m-1)}_{\text{ee}}\big]\big\},\end{aligned} \tag{8d}$$

$$\langle \boldsymbol{F}^{\text{x}(l)}_{\text{rec}}\rangle = \frac{k^{2l+2}}{c(l+1)!\,\zeta_l}\,\text{Re}\sum_{m=0}^{\lfloor\frac{l-1}{2}\rfloor} h_{l,m}\,k^{4m}\big[\bar{\eta}^{(l)}_{\text{em}}\,\boldsymbol{\varsigma}^{(l-2m)}_{\text{exm}} + \bar{\eta}^{(l)}_{\text{xx}}\,\boldsymbol{\varsigma}^{(l-2m)}_{\text{exm}} + \bar{\eta}^{(l)}_{\text{xe}}\,\boldsymbol{\varsigma}^{(l-2m)}_{\text{exe}} + \bar{\eta}^{(l)}_{\text{xm}}\,\boldsymbol{\varsigma}^{(l-2m)}_{\text{mxm}}\big], \tag{8e}$$

where the products of polarizabilities, $\eta^{(l)}_{\text{ee}}$, $\eta^{(l)}_{\text{ex}}$, $\eta^{(l)}_{\text{xx}}$ etc., are given by

$$\begin{aligned}&\eta^{(l)}_{\text{ee}} = \gamma^{(l)*}_{\text{e}}\gamma^{(l+1)}_{\text{e}},\quad \eta^{(l)}_{\text{ex}} = \gamma^{(l)*}_{\text{e}}\gamma^{(l+1)}_{\text{x}},\quad \eta^{(l)}_{\text{xe}} = \gamma^{(l)*}_{\text{x}}\gamma^{(l+1)}_{\text{e}},\quad \eta^{(l)}_{\text{xx}} = \gamma^{(l)*}_{\text{x}}\gamma^{(l+1)}_{\text{x}},\\ &\eta^{(l)}_{\text{mm}} = \gamma^{(l)*}_{\text{m}}\gamma^{(l+1)}_{\text{m}},\quad \eta^{(l)}_{\text{mx}} = \gamma^{(l)*}_{\text{m}}\gamma^{(l+1)}_{\text{x}},\quad \eta^{(l)}_{\text{xm}} = \gamma^{(l)*}_{\text{x}}\gamma^{(l+1)}_{\text{m}},\\ &\bar{\eta}^{(l)}_{\text{em}} = \gamma^{(l)*}_{\text{e}}\gamma^{(l)}_{\text{m}},\quad \bar{\eta}^{(l)}_{\text{xe}} = \gamma^{(l)*}_{\text{x}}\gamma^{(l)}_{\text{e}},\quad \bar{\eta}^{(l)}_{\text{xm}} = \gamma^{(l)*}_{\text{x}}\gamma^{(l)}_{\text{m}},\quad \bar{\eta}^{(l)}_{\text{xx}} = \gamma^{(l)*}_{\text{x}}\gamma^{(l)}_{\text{x}},\end{aligned} \tag{9}$$

and they can be written as

$$\eta^{(l)}_{\alpha\beta} = \gamma^{(l)*}_{\alpha}\gamma^{(l+1)}_{\beta},\qquad \bar{\eta}^{(l)}_{\alpha\beta} = \gamma^{(l)*}_{\alpha}\gamma^{(l)}_{\beta}, \tag{10}$$

with α, β denoting "e" or "m." The $\boldsymbol{t}$, $\boldsymbol{\tau}$, and $\boldsymbol{\varsigma}$ vectors are defined by

$$\boldsymbol{t}^{(n)}_{\text{ee}} = [\nabla^{(n)}\boldsymbol{E}^*] \overset{(n)}{\therefore} \overset{\leftrightarrow}{\mathbb{M}}^{(n)}_{\text{elec}},\quad \boldsymbol{t}^{(n)}_{\text{me}} = [\nabla^{(n)}\boldsymbol{E}^*] \overset{(n)}{\therefore} \overset{\leftrightarrow}{\mathbb{M}}^{(n)}_{\text{mag}},\quad \boldsymbol{t}^{(n)}_{\text{em}} = [\nabla^{(n)}\boldsymbol{B}^*] \overset{(n)}{\therefore} \overset{\leftrightarrow}{\mathbb{M}}^{(n)}_{\text{elec}},\quad \boldsymbol{t}^{(n)}_{\text{mm}} = [\nabla^{(n)}\boldsymbol{B}^*] \overset{(n)}{\therefore} \overset{\leftrightarrow}{\mathbb{M}}^{(n)}_{\text{mag}}, \tag{11a}$$

$$\boldsymbol{\tau}^{(n)}_{\text{ee}} = \overset{\leftrightarrow}{\mathbb{M}}^{(n)}_{\text{elec}} \overset{(n)}{\therefore} \overset{\leftrightarrow}{\mathbb{M}}^{(n+1)*}_{\text{elec}},\quad \boldsymbol{\tau}^{(n)}_{\text{me}} = \overset{\leftrightarrow}{\mathbb{M}}^{(n)}_{\text{mag}} \overset{(n)}{\therefore} \overset{\leftrightarrow}{\mathbb{M}}^{(n+1)*}_{\text{elec}},\quad \boldsymbol{\tau}^{(n)}_{\text{em}} = \overset{\leftrightarrow}{\mathbb{M}}^{(n)}_{\text{elec}} \overset{(n)}{\therefore} \overset{\leftrightarrow}{\mathbb{M}}^{(n+1)*}_{\text{mag}},\quad \boldsymbol{\tau}^{(n)}_{\text{mm}} = \overset{\leftrightarrow}{\mathbb{M}}^{(n)}_{\text{mag}} \overset{(n)}{\therefore} \overset{\leftrightarrow}{\mathbb{M}}^{(n+1)*}_{\text{mag}}, \tag{11b}$$

and

$$\varsigma^{(n)}_{\rm exm} = \Big[\overset{\leftrightarrow}{\mathbb{M}}{}^{(n)*}_{\rm elec} \overset{(n-1)}{\cdot\cdot} \overset{\leftrightarrow}{\mathbb{M}}{}^{(n)}_{\rm mag}\Big] \overset{(2)}{\cdot\cdot} \overset{\leftrightarrow}{\boldsymbol{\epsilon}},$$

$$\varsigma^{(n)}_{\rm exe} = \Big[\overset{\leftrightarrow}{\mathbb{M}}{}^{(n)*}_{\rm elec} \overset{(n-1)}{\cdot\cdot} \overset{\leftrightarrow}{\mathbb{M}}{}^{(n)}_{\rm elec}\Big] \overset{(2)}{\cdot\cdot} \overset{\leftrightarrow}{\boldsymbol{\epsilon}}, \tag{11c}$$

$$\varsigma^{(n)}_{\rm mxm} = \Big[\overset{\leftrightarrow}{\mathbb{M}}{}^{(n)*}_{\rm mag} \overset{(n-1)}{\cdot\cdot} \overset{\leftrightarrow}{\mathbb{M}}{}^{(n)}_{\rm mag}\Big] \overset{(2)}{\cdot\cdot} \overset{\leftrightarrow}{\boldsymbol{\epsilon}}.$$

In deriving Eqs. (8), we have used some mathematical identities, which, together with the coefficients $c_{l,m}$, $f_{l,m}$, $g_{l,m}$, and $h_{l,m}$, are given in Appendix B.

The decomposition of the optical force into the gradient and scattering terms is performed by splitting all the $\boldsymbol{t}$, $\boldsymbol{\tau}$, and $\boldsymbol{\varsigma}$ vectors in Eqs. (8) into the irrotational and the solenoidal parts. A vital ingredient is to write a generic monochromatic field impinging on a particle in a form similar to the angular spectrum representation [37,49],

$$\boldsymbol{E} = \oint_{4\pi} \boldsymbol{e_u}\, e^{ik\boldsymbol{u}\cdot\boldsymbol{r}}\, d\Omega_u \quad \text{and} \quad \boldsymbol{H} = \frac{1}{Z_0}\oint_{4\pi} \boldsymbol{h_u}\, e^{ik\boldsymbol{u}\cdot\boldsymbol{r}}\, d\Omega_u, \tag{12}$$

where $\boldsymbol{u}$ is the real unit vector denoting the direction of wave vector $\boldsymbol{k}$, and the integration $\oint_{4\pi}\ldots d\Omega_u$ is over the unit sphere of directions of wave vector $\boldsymbol{k} = k\,\boldsymbol{u}$. The electric and magnetic "angular spectra" $\boldsymbol{e_u}$ and $\boldsymbol{h_u}$ depend only on $\boldsymbol{u}$ (independent of $\boldsymbol{r}$) and satisfy

$$\boldsymbol{u}\cdot\boldsymbol{e_u} = \boldsymbol{u}\cdot\boldsymbol{h_u} = 0, \quad \boldsymbol{h_u} = \boldsymbol{u}\times\boldsymbol{e_u}, \quad \boldsymbol{e_u} = -\boldsymbol{u}\times\boldsymbol{h_u}. \tag{13}$$

With Eq. (12), the multiple gradients in Eq. (7) can be written as

$$\overset{\leftrightarrow}{\mathbb{M}}{}^{(n)}_{\rm elec} = \frac{(ik)^{n-1}}{n}\sum_{j=0}^{n-1}\oint_{4\pi} \boldsymbol{u}^{(n-1-j)}\,\boldsymbol{e_u}\,\boldsymbol{u}^{(j)}\,e^{ik\boldsymbol{u}\cdot\boldsymbol{r}}d\Omega_u, \tag{14a}$$

$$\overset{\leftrightarrow}{\mathbb{M}}{}^{(n)}_{\rm mag} = \frac{(ik)^{n-1}}{nc}\sum_{j=0}^{n-1}\oint_{4\pi} \boldsymbol{u}^{(n-1-j)}\,\boldsymbol{h_u}\,\boldsymbol{u}^{(j)}\,e^{ik\boldsymbol{u}\cdot\boldsymbol{r}}d\Omega_u, \tag{14b}$$

where $\boldsymbol{u}^{(n)}$ denotes the tensor product of n vectors $\boldsymbol{u}$, e.g., $\boldsymbol{u}^{(3)} = \boldsymbol{u}\otimes\boldsymbol{u}\otimes\boldsymbol{u} = \boldsymbol{u}\,\boldsymbol{u}\,\boldsymbol{u}$.

Before proceeding on, we define some field moments in reciprocal space, for integer n,

$$D^{(n)}_{\rm ee} = [\nabla^{(n-1)}\boldsymbol{E}] \overset{(n)}{\vdots} [\nabla^{(n-1)}\boldsymbol{E}^*] = k^{2n-2}\oint_{4\pi} d\Omega_u \oint_{4\pi} d\Omega_v\, (\boldsymbol{u}\cdot\boldsymbol{v})^{(n-1)}\,(\boldsymbol{e_u}\cdot\boldsymbol{e}^*_{\boldsymbol{v}})\,e^{ik(\boldsymbol{u}-\boldsymbol{v})\cdot\boldsymbol{r}},$$

$$D^{(n)}_{\rm mm} = [\nabla^{(n-1)}\boldsymbol{B}] \overset{(n)}{\vdots} [\nabla^{(n-1)}\boldsymbol{B}^*] = \frac{k^{2n-2}}{c^2}\oint_{4\pi} d\Omega_u \oint_{4\pi} d\Omega_v\, (\boldsymbol{u}\cdot\boldsymbol{v})^{n-1}\,(\boldsymbol{h_u}\cdot\boldsymbol{h}^*_{\boldsymbol{v}})\,e^{ik(\boldsymbol{u}-\boldsymbol{v})\cdot\boldsymbol{r}},$$

$$D^{(n)}_{\rm em} = [\nabla^{(n-1)}\boldsymbol{E}] \overset{(n)}{\vdots} [\nabla^{(n-1)}\boldsymbol{B}^*] = \frac{k^{2n-2}}{c}\oint_{4\pi} d\Omega_u \oint_{4\pi} d\Omega_v\, (\boldsymbol{u}\cdot\boldsymbol{v})^{n-1}\,(\boldsymbol{e_u}\cdot\boldsymbol{h}^*_{\boldsymbol{v}})\,e^{ik(\boldsymbol{u}-\boldsymbol{v})\cdot\boldsymbol{r}},$$

$$D^{(n)}_{\rm me} = [\nabla^{(n-1)}\boldsymbol{B}] \overset{(n)}{\vdots} [\nabla^{(n-1)}\boldsymbol{E}^*] = D^{(n)*}_{\rm em},$$

$$\boldsymbol{S}^{(n)}_{\rm ee} = [(\nabla^{(n-1)}\boldsymbol{E}) \overset{(n-1)}{\vdots} (\nabla^{(n-1)}\boldsymbol{E}^*)] \overset{(2)}{\vdots} \overset{\leftrightarrow}{\boldsymbol{\epsilon}} = k^{2n-2}\oint_{4\pi} d\Omega_u \oint_{4\pi} d\Omega_v\, (\boldsymbol{u}\cdot\boldsymbol{v})^{n-1}\,(\boldsymbol{e_u}\times\boldsymbol{e}^*_{\boldsymbol{v}})\,e^{ik(\boldsymbol{u}-\boldsymbol{v})\cdot\boldsymbol{r}},$$

$$\boldsymbol{S}^{(n)}_{\rm mm} = [(\nabla^{(n-1)}\boldsymbol{B}) \overset{(n-1)}{\vdots} (\nabla^{(n-1)}\boldsymbol{B}^*)] \overset{(2)}{\vdots} \overset{\leftrightarrow}{\boldsymbol{\epsilon}} = \frac{k^{2n-2}}{c^2}\oint_{4\pi} d\Omega_u \oint_{4\pi} d\Omega_v\, (\boldsymbol{u}\cdot\boldsymbol{v})^{n-1}\,(\boldsymbol{h_u}\times\boldsymbol{h}^*_{\boldsymbol{v}})\,e^{ik(\boldsymbol{u}-\boldsymbol{v})\cdot\boldsymbol{r}},$$

$$\boldsymbol{S}^{(n)}_{\rm em} = [(\nabla^{(n-1)}\boldsymbol{E}) \overset{(n-1)}{\vdots} (\nabla^{(n-1)}\boldsymbol{B}^*)] \overset{(2)}{\vdots} \overset{\leftrightarrow}{\boldsymbol{\epsilon}} = \frac{k^{2n-2}}{c}\oint_{4\pi} d\Omega_u \oint_{4\pi} d\Omega_v\, (\boldsymbol{u}\cdot\boldsymbol{v})^{n-1}\,(\boldsymbol{e_u}\times\boldsymbol{h}^*_{\boldsymbol{v}})\,e^{ik(\boldsymbol{u}-\boldsymbol{v})\cdot\boldsymbol{r}},$$

$$\boldsymbol{S}^{(n)}_{\rm me} = [(\nabla^{(n-1)}\boldsymbol{B}) \overset{(n-1)}{\vdots} (\nabla^{(n-1)}\boldsymbol{E}^*)] \overset{(2)}{\vdots} \overset{\leftrightarrow}{\boldsymbol{\epsilon}} = -\boldsymbol{S}^{(n)*}_{\rm em},$$

$$\boldsymbol{G}^{(n)}_{\rm ee} = [\nabla^{(n-1)}\boldsymbol{E}] \overset{(n)}{\vdots} [\nabla^{(n)}\boldsymbol{E}^*] = -ik^{2n-1}\oint_{4\pi} d\Omega_u \oint_{4\pi} d\Omega_v\, (\boldsymbol{u}\cdot\boldsymbol{v})^{n-1}\,(\boldsymbol{e_u}\cdot\boldsymbol{v})\,\boldsymbol{e}^*_{\boldsymbol{v}}\,e^{ik(\boldsymbol{u}-\boldsymbol{v})\cdot\boldsymbol{r}},$$

$$\boldsymbol{G}^{(n)}_{\rm mm} = [\nabla^{(n-1)}\boldsymbol{B}] \overset{(n)}{\vdots} [\nabla^{(n)}\boldsymbol{B}^*] = -\frac{ik^{2n-1}}{c^2}\oint_{4\pi} d\Omega_u \oint_{4\pi} d\Omega_v\, (\boldsymbol{u}\cdot\boldsymbol{v})^{n-1}\,(\boldsymbol{h_u}\cdot\boldsymbol{v})\,\boldsymbol{h}^*_{\boldsymbol{v}}\,e^{ik(\boldsymbol{u}-\boldsymbol{v})\cdot\boldsymbol{r}},$$

$$\begin{aligned}
\boldsymbol{G}_{\mathrm{em}}^{(n)} &= [\nabla^{(n-1)}\boldsymbol{E}] \overset{(n)}{\vdots} [\nabla^{(n)}\boldsymbol{B}^*] = -\frac{ik^{2n-1}}{c}\oint_{4\pi} d\Omega_u \oint_{4\pi} d\Omega_v\, (\boldsymbol{u}\cdot\boldsymbol{v})^{n-1}\,(\boldsymbol{e}_{\boldsymbol{u}}\cdot\boldsymbol{v})\,\boldsymbol{h}_{\boldsymbol{v}}^*\, e^{ik(\boldsymbol{u}-\boldsymbol{v})\cdot\boldsymbol{r}},\\
\boldsymbol{G}_{\mathrm{me}}^{(n)} &= [\nabla^{(n-1)}\boldsymbol{B}] \overset{(n)}{\vdots} [\nabla^{(n)}\boldsymbol{E}^*] = -\frac{ik^{2n-1}}{c}\oint_{4\pi} d\Omega_u \oint_{4\pi} d\Omega_v\, (\boldsymbol{u}\cdot\boldsymbol{v})^{n-1}\,(\boldsymbol{h}_{\boldsymbol{u}}\cdot\boldsymbol{v})\,\boldsymbol{e}_{\boldsymbol{v}}^*\, e^{ik(\boldsymbol{u}-\boldsymbol{v})\cdot\boldsymbol{r}},
\end{aligned}\tag{15}$$

where $n \geqslant 1$ and the tensor contraction $\overset{(n)}{\vdots}$ is defined as follows,

$$\overset{\leftrightarrow}{\mathbb{A}}^{(l)} \overset{(m)}{\vdots} \overset{\leftrightarrow}{\mathbb{B}}^{(l')} = \mathbb{A}^{(l)}_{k_1 k_2 \ldots k_m i_{m+1} i_{m+2} \ldots i_l}\, \mathbb{B}^{(l')}_{k_1 k_2 \ldots k_m j_{m+1} j_{m+2} \ldots j_{l'}}, \quad 0 \leqslant m \leqslant \min[l, l'];\tag{16}$$

that is, the tensor contraction is successively made over the corresponding left-most indices in the two index sequences, which differs from $\overset{(n)}{\because}$ defined in Eq. (3) with the tensor contraction being consecutively made over two nearest indices. Some simple examples are, for any vectors $\boldsymbol{v}$ and $\boldsymbol{w}$,

$$\begin{aligned}
&(\boldsymbol{v}\boldsymbol{w}) \overset{(2)}{\because} \overset{\leftrightarrow}{\boldsymbol{\epsilon}} = v_j w_i \epsilon_{ijk} = \boldsymbol{w}\times\boldsymbol{v} \quad \text{versus} \quad (\boldsymbol{v}\boldsymbol{w}) \overset{(2)}{\vdots} \overset{\leftrightarrow}{\boldsymbol{\epsilon}} = v_i w_j \epsilon_{ijk} = \boldsymbol{v}\times\boldsymbol{w},\\
&(\nabla\nabla\boldsymbol{v}) \overset{(2)}{\because} (\nabla\boldsymbol{w}) = (\partial_i\partial_j v_k)(\partial_k w_j) \quad \text{versus} \quad (\nabla\nabla\boldsymbol{v}) \overset{(2)}{\vdots} (\nabla\boldsymbol{w}) = (\partial_i\partial_j v_k)(\partial_i w_j),\\
&(\nabla\boldsymbol{w}) \overset{(2)}{\because} (\nabla\nabla\boldsymbol{v}) = (\partial_i w_j)(\partial_j\partial_i v_k) \quad \text{versus} \quad (\nabla\boldsymbol{w}) \overset{(2)}{\vdots} (\nabla\nabla\boldsymbol{v}) = (\partial_i w_j)(\partial_i\partial_j v_k),
\end{aligned}\tag{17}$$

with v_j (w_j) denoting the jth Cartesian component of the vector $\boldsymbol{v}$ ($\boldsymbol{w}$). It can be demonstrated that the field moments defined in Eq. (15) satisfy

$$\nabla\cdot\boldsymbol{S}_{\mathrm{ee}}^{(n)} = 2i\omega\,\mathrm{Re}\big[D_{\mathrm{em}}^{(n)}\big], \quad \nabla\cdot\boldsymbol{S}_{\mathrm{mm}}^{(n)} = -\frac{2i\omega}{c^2}\,\mathrm{Re}\big[D_{\mathrm{em}}^{(n)}\big], \quad \nabla\cdot\mathrm{Re}\,\boldsymbol{S}_{\mathrm{em}}^{(n)} = 0,\tag{18}$$

and many other relations given in Appendix C.

After lengthy algebra, one can re-express the $\boldsymbol{t}$, $\boldsymbol{\tau}$, and $\boldsymbol{\varsigma}$ vectors in Eqs. (11) by field moments D, $\boldsymbol{S}$, and $\boldsymbol{G}$ defined in Eq. (15). The $\boldsymbol{t}$ vectors in Eq. (11a) for the partial extinction forces $\langle\boldsymbol{F}_{\mathrm{int}}^{\mathrm{e}(l)}\rangle$ and $\langle\boldsymbol{F}_{\mathrm{int}}^{\mathrm{m}(l)}\rangle$ on order-l electric and magnetic multipoles (2^l-poles) are rewritten as

$$\begin{aligned}
\boldsymbol{t}_{\mathrm{ee}}^{(n)} &= \boldsymbol{Z}_{\mathrm{ee}}^{(n)} - \frac{(n-1)k^2c^2}{n}\boldsymbol{Z}_{\mathrm{mm}}^{(n-1)}, \quad \boldsymbol{t}_{\mathrm{mm}}^{(n)} = \boldsymbol{Z}_{\mathrm{mm}}^{(n)} - \frac{(n-1)k^2}{n\,c^2}\boldsymbol{Z}_{\mathrm{ee}}^{(n-1)},\\
\boldsymbol{t}_{\mathrm{me}}^{(n)} &= \boldsymbol{Z}_{\mathrm{me}}^{(n)} + \frac{(n-1)k^2}{n}\boldsymbol{Z}_{\mathrm{em}}^{(n-1)}, \quad \boldsymbol{t}_{\mathrm{em}}^{(n)} = \boldsymbol{Z}_{\mathrm{em}}^{(n)} + \frac{(n-1)k^2}{n}\boldsymbol{Z}_{\mathrm{me}}^{(n-1)},
\end{aligned}\tag{19}$$

where

$$\begin{aligned}
\boldsymbol{Z}_{\mathrm{ee}}^{(n)} &= \frac{1}{2}\big[\nabla D_{\mathrm{ee}}^{(n)} - \nabla\times\boldsymbol{S}_{\mathrm{ee}}^{(n)} - 2ikc\,\mathrm{Re}\,\boldsymbol{S}_{\mathrm{em}}^{(n)}\big],\\
\boldsymbol{Z}_{\mathrm{mm}}^{(n)} &= \frac{1}{2}\left[\nabla D_{\mathrm{mm}}^{(n)} - \nabla\times\boldsymbol{S}_{\mathrm{mm}}^{(n)} - \frac{2ik}{c}\,\mathrm{Re}\,\boldsymbol{S}_{\mathrm{em}}^{(n)}\right],\\
\boldsymbol{Z}_{\mathrm{me}}^{(n)} &= \frac{1}{2}\left[\nabla D_{\mathrm{me}}^{(n)} - \nabla\times\boldsymbol{S}_{\mathrm{me}}^{(n)} - \frac{ik}{c}\big(\boldsymbol{S}_{\mathrm{ee}}^{(n)} + c^2\boldsymbol{S}_{\mathrm{mm}}^{(n)}\big)\right],\\
\boldsymbol{Z}_{\mathrm{em}}^{(n)} &= \frac{1}{2}\left[\nabla D_{\mathrm{em}}^{(n)} - \nabla\times\boldsymbol{S}_{\mathrm{em}}^{(n)} + \frac{ik}{c}\big(\boldsymbol{S}_{\mathrm{ee}}^{(n)} + c^2\boldsymbol{S}_{\mathrm{mm}}^{(n)}\big)\right],
\end{aligned}\tag{20}$$

and use has been made of $D_{\mathrm{me}}^{(n)} = D_{\mathrm{em}}^{(n)*}$, $\boldsymbol{S}_{\mathrm{me}}^{(n)} = -\boldsymbol{S}_{\mathrm{em}}^{(n)*}$, and $\nabla\times\mathrm{Im}\,[\boldsymbol{G}_{\mathrm{ee}}^{(n-1)} + c^2\boldsymbol{G}_{\mathrm{mm}}^{(n-1)}] = -i\,[\boldsymbol{S}_{\mathrm{ee}}^{(n)} + c^2\boldsymbol{S}_{\mathrm{mm}}^{(n)}] + ik^2[\boldsymbol{S}_{\mathrm{ee}}^{(n-1)} + c^2\boldsymbol{S}_{\mathrm{mm}}^{(n-1)}]$ given in Eqs. (18). Equations (19) and (20) are readily in a decomposed form, since $\nabla\cdot\mathrm{Re}\,\boldsymbol{S}_{\mathrm{em}}^{(n)} = 0$ and $\nabla\cdot[\boldsymbol{S}_{\mathrm{ee}}^{(n)} + c^2\boldsymbol{S}_{\mathrm{mm}}^{(n)}] = 0$, which follows Eqs. (18). The $\boldsymbol{\tau}$ vectors defined in Eq. (11b) and appearing in the electric and magnetic parts of the recoil force, as described by Eqs. (8c) and (8d), can be derived in a similar way, leading to

$$\boldsymbol{\tau}_{\mathrm{ee}}^{(n)} = \boldsymbol{Z}_{\mathrm{ee}}^{(n)} - \frac{(n-1)k^2c^2}{(n+1)}\boldsymbol{Z}_{\mathrm{mm}}^{(n-1)} + \frac{ikc}{(n+1)}\boldsymbol{S}_{\mathrm{em}}^{(n)},\tag{21a}$$

$$\boldsymbol{\tau}_{\mathrm{mm}}^{(n)} = \boldsymbol{Z}_{\mathrm{mm}}^{(n)} - \frac{(n-1)k^2}{(n+1)c^2}\boldsymbol{Z}_{\mathrm{ee}}^{(n-1)} + \frac{ik}{(n+1)c}\boldsymbol{S}_{\mathrm{em}}^{(n)*},\tag{21b}$$

$$\boldsymbol{\tau}_{\mathrm{em}}^{(n)} = \boldsymbol{Z}_{\mathrm{em}}^{(n)} + \frac{(n-1)k^2}{(n+1)}\boldsymbol{Z}_{\mathrm{me}}^{(n-1)} - \frac{ik}{(n+1)c}\boldsymbol{S}_{\mathrm{ee}}^{(n)},\tag{21c}$$

$$\boldsymbol{\tau}_{\mathrm{me}}^{(n)} = \boldsymbol{Z}_{\mathrm{me}}^{(n)} + \frac{(n-1)k^2}{(n+1)}\boldsymbol{Z}_{\mathrm{em}}^{(n-1)} + \frac{ikc}{(n+1)}\boldsymbol{S}_{\mathrm{mm}}^{(n)}.\tag{21d}$$

The ς vectors in the hybrid recoil term $\langle \boldsymbol{F}_{\rm rec}^{\rm x(\mathit{l})}\rangle$ given by Eq. (8e) turn out to be most complicated. They can be eventually cast, based on the definition Eq. (11c), into

$$\begin{aligned}\varsigma_{\rm exm}^{(n)} =& \frac{i\,(n-1)k}{n\,c}\left[\boldsymbol{Z}_{\rm ee}^{(n-1)} - c^2\boldsymbol{Z}_{\rm mm}^{(n-1)*}\right] + \frac{i\,(n-1)(n-2)k^3}{n^2c}\left[\boldsymbol{Z}_{\rm ee}^{(n-2)*} - c^2\boldsymbol{Z}_{\rm mm}^{(n-2)}\right]\\ &-\boldsymbol{S}_{\rm em}^{(n)*} - \frac{(n-1)k^2}{n^2}\boldsymbol{S}_{\rm em}^{(n-1)} + \frac{(n-1)(n-2)k^4}{n^2}\boldsymbol{S}_{\rm em}^{(n-2)*}, \end{aligned}\tag{22a}$$

$$\begin{aligned}\varsigma_{\rm exe}^{(n)} =& -\frac{i\,(n-1)kc}{n}\left[\boldsymbol{Z}_{\rm me}^{(n-1)} + \boldsymbol{Z}_{\rm me}^{(n-1)*}\right] - \frac{i\,(n-1)(n-2)k^3c}{n^2}\left[\boldsymbol{Z}_{\rm em}^{(n-2)*} + \boldsymbol{Z}_{\rm em}^{(n-2)}\right]\\ &+\boldsymbol{S}_{\rm ee}^{(n)} + \frac{(n-1)k^2c^2}{n^2}\boldsymbol{S}_{\rm mm}^{(n-1)} - \frac{(n-1)(n-2)k^4}{n^2}\boldsymbol{S}_{\rm ee}^{(n-2)}, \end{aligned}\tag{22b}$$

$$\begin{aligned}\varsigma_{\rm mxm}^{(n)} =& \frac{i\,(n-1)k}{nc}\left[\boldsymbol{Z}_{\rm em}^{(n-1)} + \boldsymbol{Z}_{\rm em}^{(n-1)*}\right] + \frac{i\,(n-1)(n-2)k^3}{n^2c}\left[\boldsymbol{Z}_{\rm me}^{(n-2)*} + \boldsymbol{Z}_{\rm me}^{(n-2)}\right]\\ &+\boldsymbol{S}_{\rm mm}^{(n)} + \frac{(n-1)k^2}{n^2c^2}\boldsymbol{S}_{\rm ee}^{(n-1)} - \frac{(n-1)(n-2)k^4}{n^2}\boldsymbol{S}_{\rm mm}^{(n-2)}. \end{aligned}\tag{22c}$$

The recoil force $\langle \boldsymbol{F}_{\rm rec}^{(l)}\rangle$, given by Eqs. (8c)–(8e) and dependent on the vectors $\boldsymbol{\tau}$ and ς, still entangles with the conservative and nonconservative forces because the $\boldsymbol{S}$ vectors are neither irrotational and solenoidal. Since all the $\boldsymbol{Z}$ vectors [see Eq. (20)] have been partitioned, the last step for dividing optical force into the conservative and nonconservative parts relies on partitioning $\boldsymbol{S}_{\rm ee}^{(n)}$, $\boldsymbol{S}_{\rm mm}^{(n)}$, and $\boldsymbol{S}_{\rm em}^{(n)}$. It can be derived (see Appendix D for the details) that

$$\boldsymbol{S}_{\rm ee}^{(n)} = -\frac{i\,c}{k}\nabla\sum_{m=0}^{\infty}\frac{1}{k^{2m}}\,{\rm Re}\,D_{\rm em}^{(n+m)} - \frac{i}{k^2}\nabla\times\sum_{m=0}^{\infty}\frac{1}{k^{2m}}\,{\rm Im}\,\boldsymbol{G}_{\rm ee}^{(n+m)} + \boldsymbol{S}_{\rm ee}^{(n)}\big|_{\boldsymbol{u}=\boldsymbol{v}},\tag{23a}$$

$$\boldsymbol{S}_{\rm mm}^{(n)} = \frac{i}{kc}\nabla\sum_{m=0}^{\infty}\frac{1}{k^{2m}}\,{\rm Re}\,D_{\rm em}^{(n+m)} - \frac{i}{k^2}\nabla\times\sum_{m=0}^{\infty}\frac{1}{k^{2m}}\,{\rm Im}\,\boldsymbol{G}_{\rm mm}^{(n+m)} + \boldsymbol{S}_{\rm mm}^{(n)}\big|_{\boldsymbol{u}=\boldsymbol{v}},\tag{23b}$$

$$\begin{aligned}\boldsymbol{S}_{\rm em}^{(n)} =& -\frac{i}{2kc}\nabla\sum_{m=0}^{\infty}\frac{1}{k^{2m}}\left[c^2D_{\rm mm}^{(n+m)} - D_{\rm ee}^{(n+m)}\right]\\ &-\frac{1}{2k^2}\nabla\times\sum_{m=0}^{\infty}\frac{1}{k^{2m}}\left[\boldsymbol{G}_{\rm em}^{(n+m)} - \boldsymbol{G}_{\rm me}^{(n+m)*}\right] + \boldsymbol{S}_{\rm em}^{(n)}\big|_{\boldsymbol{u}=\boldsymbol{v}}, \end{aligned}\tag{23c}$$

where, following Eq. (15), the last terms on the right-hand sides are constant vectors reading

$$\begin{aligned}&\boldsymbol{S}_{\rm ee}^{(n)}\big|_{\boldsymbol{u}=\boldsymbol{v}} = k^{2n-2}\oint_{4\pi}(\boldsymbol{e}_{\boldsymbol{u}}\times\boldsymbol{e}_{\boldsymbol{u}}^*)d\Omega_u,\quad \boldsymbol{S}_{\rm mm}^{(n)}\big|_{\boldsymbol{u}=\boldsymbol{v}} = \frac{k^{2n-2}}{c^2}\oint_{4\pi}(\boldsymbol{h}_{\boldsymbol{u}}\times\boldsymbol{h}_{\boldsymbol{u}}^*)d\Omega_u,\\ &\boldsymbol{S}_{\rm em}^{(n)}\big|_{\boldsymbol{u}=\boldsymbol{v}} = \frac{k^{2n-2}}{c}\oint_{4\pi}(\boldsymbol{e}_{\boldsymbol{u}}\times\boldsymbol{h}_{\boldsymbol{u}}^*)d\Omega_u = \frac{k^{2n-2}}{c}\oint_{4\pi}|\,\boldsymbol{e}_{\boldsymbol{u}}|^2\boldsymbol{u}\,d\Omega_u. \end{aligned}\tag{24}$$

The constant vectors in Eq. (24) make position-independent constant contributions to optical force. To be consistent with the concept of radiation (scattering) force on a particle under the illumination of a single plane wave, we choose to attribute these contributions entirely to the solenoidal part of the optical force in our treatment. Furthermore, the position-independent constant force should belong to scattering force, because it takes an infinitely large potential energy to produce it if it is a gradient force. As a consequence, Eqs. (23) complete the decomposition of $\boldsymbol{S}_{\rm ee}^{(n)}$, $\boldsymbol{S}_{\rm mm}^{(n)}$, and $\boldsymbol{S}_{\rm em}^{(n)}$ into the solenoidal and irrotational parts.

We have therefore concluded the formulations of optical force and its two decomposed parts, conservative force and nonconservative force, or, say, gradient force and scattering force, within the framework of Cartesian multipole expansion theory for optical force.

C. Optical force and its decomposition for multiple interferential plane-wave fields

Any monochromatic optical field can be expressed as an integral over homogeneous plane-wave spectrum [49–53]. As the integral can be evaluated by summation, generic monochromatic optical fields may then be written, up to arbitrary accuracy, as a discrete spectrum of homogeneous plane waves. In this subsection, based on the formulations for optical force within the Cartesian multipole expansion theory proposed in the last subsection, we will derive a set of explicit analytical expressions to calculate the optical force and, in particular, its two partitioned parts, acting on a spherical chiral particle immersed in multiple interferential plane waves fields. As generic optical fields can be depicted by a superposition of discrete homogeneous plane waves, our approach works indeed for any monochromatic optical field.

Written in terms of multiple interferential plane waves, the electric and magnetic fields of a generic optical field can be cast into

$$\boldsymbol{E} = \sum_{i=1}^{n_p} \boldsymbol{E}_i = \sum_{i=1}^{n_p} \boldsymbol{\mathcal{E}}_i e^{i k \hat{\boldsymbol{k}}_i \cdot \boldsymbol{r}}, \qquad \boldsymbol{B} = \sum_{i=1}^{n_p} \boldsymbol{B}_i = \sum_{i=1}^{n_p} \boldsymbol{\mathcal{B}}_i e^{i k \hat{\boldsymbol{k}}_i \cdot \boldsymbol{r}}, \tag{25}$$

where $k = \omega/c$, $\hat{\boldsymbol{k}}_i$ is the unit vector denoting the direction of the (real) wave vector $\boldsymbol{k}_i = k\hat{\boldsymbol{k}}_i$ of the ith plane wave in the lossless background, n_p is the number of the plane waves making up the optical fields, and $\boldsymbol{\mathcal{E}}_i$ and $\boldsymbol{\mathcal{B}}_i = \boldsymbol{k}_i \times \boldsymbol{\mathcal{E}}_i$ are complex amplitude vectors of the ith plane wave. Substituting the field expressions Eqs. (25) into Eq. (15), all the field moments defined for total field share the following form,

$$\boldsymbol{X}^{(n)} = \sum_{i=1}^{n_p} \sum_{j=1}^{n_p} \boldsymbol{X}_{ij}^{(n)}, \tag{26}$$

which are written as a sum over field moments $\boldsymbol{X}_{ij}^{(n)}$ for each pair of plane waves, termed pair representation below. To be specific, the field moments for any pair (i, j) of the plane waves are given by

$$\begin{aligned}
D_{\mathrm{ee},\,ij}^{(n)} &= (\boldsymbol{k}_i \cdot \boldsymbol{k}_j)^{n-1} (\boldsymbol{\mathcal{E}}_i \cdot \boldsymbol{\mathcal{E}}_j^*)\, e^{i(\boldsymbol{k}_i - \boldsymbol{k}_j)\cdot \boldsymbol{r}}, \quad D_{\mathrm{mm},\,ij}^{(n)} = (\boldsymbol{k}_i \cdot \boldsymbol{k}_j)^{n-1} (\boldsymbol{\mathcal{B}}_i \cdot \boldsymbol{\mathcal{B}}_j^*)\, e^{i(\boldsymbol{k}_i - \boldsymbol{k}_j)\cdot \boldsymbol{r}},\\
D_{\mathrm{em},\,ij}^{(n)} &= (\boldsymbol{k}_i \cdot \boldsymbol{k}_j)^{n-1} (\boldsymbol{\mathcal{E}}_i \cdot \boldsymbol{\mathcal{B}}_j^*)\, e^{i(\boldsymbol{k}_i - \boldsymbol{k}_j)\cdot \boldsymbol{r}}, \quad D_{\mathrm{me},\,ij}^{(n)} = (\boldsymbol{k}_i \cdot \boldsymbol{k}_j)^{n-1} (\boldsymbol{\mathcal{B}}_i \cdot \boldsymbol{\mathcal{E}}_j^*)\, e^{i(\boldsymbol{k}_i - \boldsymbol{k}_j)\cdot \boldsymbol{r}},\\
\boldsymbol{S}_{\mathrm{ee},ij}^{(n)} &= (\boldsymbol{k}_i \cdot \boldsymbol{k}_j)^{n-1} (\boldsymbol{\mathcal{E}}_i \times \boldsymbol{\mathcal{E}}_j^*)\, e^{i(\boldsymbol{k}_i - \boldsymbol{k}_j)\cdot \boldsymbol{r}}, \quad \boldsymbol{S}_{\mathrm{mm},\,ij}^{(n)} = (\boldsymbol{k}_i \cdot \boldsymbol{k}_j)^{n-1} (\boldsymbol{\mathcal{B}}_i \times \boldsymbol{\mathcal{B}}_j^*)\, e^{i(\boldsymbol{k}_i - \boldsymbol{k}_j)\cdot \boldsymbol{r}},\\
\boldsymbol{S}_{\mathrm{em},\,ij}^{(n)} &= (\boldsymbol{k}_i \cdot \boldsymbol{k}_j)^{n-1} (\boldsymbol{\mathcal{E}}_i \times \boldsymbol{\mathcal{B}}_j^*)\, e^{i(\boldsymbol{k}_i - \boldsymbol{k}_j)\cdot \boldsymbol{r}}, \quad \boldsymbol{S}_{\mathrm{me},\,ij}^{(n)} = (\boldsymbol{k}_i \cdot \boldsymbol{k}_j)^{n-1} (\boldsymbol{\mathcal{B}}_i \times \boldsymbol{\mathcal{E}}_j^*)\, e^{i(\boldsymbol{k}_i - \boldsymbol{k}_j)\cdot \boldsymbol{r}},\\
\boldsymbol{G}_{\mathrm{ee},\,ij}^{(n)} &= -i\,(\boldsymbol{k}_i \cdot \boldsymbol{k}_j)^{n-1} (\boldsymbol{k}_j \cdot \boldsymbol{\mathcal{E}}_i)\, \boldsymbol{\mathcal{E}}_j^*\, e^{i(\boldsymbol{k}_i - \boldsymbol{k}_j)\cdot \boldsymbol{r}}, \quad \boldsymbol{G}_{\mathrm{mm},\,ij}^{(n)} = -i\,(\boldsymbol{k}_i \cdot \boldsymbol{k}_j)^{n-1} (\boldsymbol{k}_j \cdot \boldsymbol{\mathcal{B}}_i)\, \boldsymbol{\mathcal{B}}_j^*\, e^{i(\boldsymbol{k}_i - \boldsymbol{k}_j)\cdot \boldsymbol{r}},\\
\boldsymbol{G}_{\mathrm{em},\,ij}^{(n)} &= -i\,(\boldsymbol{k}_i \cdot \boldsymbol{k}_j)^{n-1} (\boldsymbol{k}_j \cdot \boldsymbol{\mathcal{E}}_i)\, \boldsymbol{\mathcal{B}}_j^*\, e^{i(\boldsymbol{k}_i - \boldsymbol{k}_j)\cdot \boldsymbol{r}}, \quad \boldsymbol{G}_{\mathrm{me},\,ij}^{(n)} = -i\,(\boldsymbol{k}_i \cdot \boldsymbol{k}_j)^{n-1} (\boldsymbol{k}_j \cdot \boldsymbol{\mathcal{B}}_i)\, \boldsymbol{\mathcal{E}}_j^*\, e^{i(\boldsymbol{k}_i - \boldsymbol{k}_j)\cdot \boldsymbol{r}}.
\end{aligned} \tag{27}$$

It is noted that all terms are constants when $i = j$. In pair representation, any quantity in Eqs. (27) have the form

$$\boldsymbol{X}_{ij}^{(n)} = k^{2n-2} x_{ij}^{n-1} \boldsymbol{X}_{ij}^{(1)}, \tag{28}$$

which simplifies $\boldsymbol{X}_{ij}^{(n)}$ to $\boldsymbol{X}_{ij}^{(1)}$, with $x_{ij} = \hat{\boldsymbol{k}}_i \cdot \hat{\boldsymbol{k}}_j$. Substituting Eqs. (26)–(28) into Eq. (20), we have the $\boldsymbol{Z}$ vectors reduced to

$$\boldsymbol{Z}^{(n)} = \sum_{i,\,j} \boldsymbol{Z}_{ij}^{(n)} = \sum_{i,\,j} k^{2n-2} x_{ij}^{n-1} \boldsymbol{Z}_{ij}^{(1)}, \tag{29}$$

with, explicitly,

$$\begin{aligned}
\boldsymbol{Z}_{\mathrm{ee},ij}^{(1)} &= \tfrac{1}{2}\big[\nabla D_{\mathrm{ee},ij}^{(1)} - \nabla \times \boldsymbol{S}_{\mathrm{ee},ij}^{(1)} - 2ik\,\mathrm{Re}\,\boldsymbol{S}_{\mathrm{em},ij}^{(1)}\big], \quad \boldsymbol{Z}_{\mathrm{mm},ij}^{(1)} = \tfrac{1}{2}\big[\nabla D_{\mathrm{mm},ij}^{(1)} - \nabla \times \boldsymbol{S}_{\mathrm{mm},ij}^{(1)} - 2ik\,\mathrm{Re}\,\boldsymbol{S}_{\mathrm{em},ij}^{(1)}\big],\\
\boldsymbol{Z}_{\mathrm{me},ij}^{(1)} &= \tfrac{1}{2}\big[\nabla D_{\mathrm{me},ij}^{(1)} - \nabla \times \boldsymbol{S}_{\mathrm{me},ij}^{(1)} - ik\big(\boldsymbol{S}_{\mathrm{ee},ij}^{(1)} + \boldsymbol{S}_{\mathrm{mm},ij}^{(1)}\big)\big], \quad \boldsymbol{Z}_{\mathrm{em},ij}^{(1)} = \tfrac{1}{2}\big[\nabla D_{\mathrm{em},ij}^{(1)} - \nabla \times \boldsymbol{S}_{\mathrm{em},ij}^{(1)} + ik\big(\boldsymbol{S}_{\mathrm{ee},ij}^{(1)} + \boldsymbol{S}_{\mathrm{mm},ij}^{(1)}\big)\big].
\end{aligned} \tag{30}$$

Similar expressions can be obtained for the $\boldsymbol{S}$ vectors. In this subsection, we use electrodynamic units with $\varepsilon_0 = \mu_0 = c = 1$ for simplicity. Inserting the expressions of the $\boldsymbol{Z}$ vectors Eq. (29) together with the similar expressions for the $\boldsymbol{S}$ vectors into Eqs. (19), (21), and (22), one can rewrite the $\boldsymbol{t}$, $\boldsymbol{\tau}$ and $\boldsymbol{\varsigma}$ vectors in terms of the $\boldsymbol{Z}$ and $\boldsymbol{S}$ vectors in pair representation, which, when plugged into the forces equations Eq. (8), eventually give rise to

$$\begin{aligned}
\big\langle \boldsymbol{F}_{\mathrm{int}}^{\mathrm{e}(l)} \big\rangle &= -\frac{\pi\,(2l+1)}{l\,(l+1)} \sum_{i,\,j} \big\{\mathrm{Im}\big[a_l\, \boldsymbol{Y}_{l,ij}^{(1)}\big] + \mathrm{Re}\big[c_l\, \boldsymbol{Y}_{l,ij}^{(2)}\big]\big\}, \quad \big\langle \boldsymbol{F}_{\mathrm{int}}^{\mathrm{m}(l)} \big\rangle = -\frac{\pi\,(2l+1)}{l\,(l+1)} \sum_{i,\,j} \big\{\mathrm{Im}\big[b_l\, \boldsymbol{Y}_{l,ij}^{(3)}\big] - \mathrm{Re}\big[c_l\, \boldsymbol{Y}_{l,ij}^{(4)}\big]\big\},\\
\big\langle \boldsymbol{F}_{\mathrm{rec}}^{\mathrm{e}(l)} \big\rangle &= -\frac{\pi}{2\,(l+1)^2} \sum_{i,\,j} \mathrm{Im}\big[a_l^* a_{l+1} \boldsymbol{Y}_{l,ij}^{(5)} + i\, a_l^* c_{l+1} \boldsymbol{Y}_{l,ij}^{(6)} - i\, c_l^* a_{l+1} \boldsymbol{Y}_{l,ij}^{(7)} + c_l^* c_{l+1} \boldsymbol{Y}_{l,ij}^{(8)}\big],\\
\big\langle \boldsymbol{F}_{\mathrm{rec}}^{\mathrm{m}(l)} \big\rangle &= -\frac{\pi}{2\,(l+1)^2} \sum_{i,\,j} \mathrm{Im}\big[b_l^* b_{l+1} \boldsymbol{Y}_{l,ij}^{(8)} - i\, b_l^* c_{l+1} \boldsymbol{Y}_{l,ij}^{(7)} + i\, c_l^* b_{l+1} \boldsymbol{Y}_{l,ij}^{(6)} + c_l^* c_{l+1} \boldsymbol{Y}_{l,ij}^{(5)}\big],\\
\big\langle \boldsymbol{F}_{\mathrm{rec}}^{\mathrm{x}(l)} \big\rangle &= \frac{\pi\,(2l+1)}{2\,l^2\,(l+1)^2} \sum_{i,\,j} \mathrm{Re}\big[a_l^* b_l \boldsymbol{Y}_{l,ij}^{(9)} + c_l^* c_l \boldsymbol{Y}_{l,ij}^{(9)} - c_l^* a_l \boldsymbol{Y}_{l,ij}^{(10)} + c_l^* b_l \boldsymbol{Y}_{l,ij}^{(11)}\big],
\end{aligned} \tag{31}$$

where

$$\begin{aligned}
\boldsymbol{Y}_{l,ij}^{(1)} &= Q_{l,ij}^{(1)} \boldsymbol{Z}_{\mathrm{ee},ij}^{(1)} - Q_{l,ij}^{(2)} \boldsymbol{Z}_{\mathrm{mm},ij}^{(1)}, \quad \boldsymbol{Y}_{l,ij}^{(2)} = Q_{l,ij}^{(1)} \boldsymbol{Z}_{\mathrm{me},ij}^{(1)} + Q_{l,ij}^{(2)} \boldsymbol{Z}_{\mathrm{em},ij}^{(1)},\\
\boldsymbol{Y}_{l,ij}^{(3)} &= Q_{l,ij}^{(1)} \boldsymbol{Z}_{\mathrm{mm},ij}^{(1)} - Q_{l,ij}^{(2)} \boldsymbol{Z}_{\mathrm{ee},ij}^{(1)}, \quad \boldsymbol{Y}_{l,ij}^{(4)} = Q_{l,ij}^{(1)} \boldsymbol{Z}_{\mathrm{em},ij}^{(1)} + Q_{l,ij}^{(2)} \boldsymbol{Z}_{\mathrm{me},ij}^{(1)},
\end{aligned}$$

$$\begin{aligned}
\boldsymbol{Y}^{(5)}_{l,ij} &= R^{(1)}_{l,ij}\boldsymbol{Z}^{(1)*}_{\mathrm{ee},ij} - R^{(2)}_{l,ij}\boldsymbol{Z}^{(1)*}_{\mathrm{mm},ij} - 4i\,k\,R^{(3)}_{l,ij}\boldsymbol{S}^{(1)*}_{\mathrm{em},ij} + R^{(4)}_{l,ij}\boldsymbol{Z}^{(1)}_{\mathrm{ee},ij} - R^{(5)}_{l,ij}\boldsymbol{Z}^{(1)}_{\mathrm{mm},ij} + 4i\,k\,R^{(6)}_{l,ij}\boldsymbol{S}^{(1)}_{\mathrm{em},ij},\\
\boldsymbol{Y}^{(6)}_{l,ij} &= R^{(1)}_{l,ij}\boldsymbol{Z}^{(1)*}_{\mathrm{em},ij} + R^{(2)}_{l,ij}\boldsymbol{Z}^{(1)*}_{\mathrm{me},ij} + 4i\,k\,R^{(3)}_{l,ij}\boldsymbol{S}^{(1)*}_{\mathrm{ee},ij} + R^{(4)}_{l,ij}\boldsymbol{Z}^{(1)}_{\mathrm{me},ij} + R^{(5)}_{l,ij}\boldsymbol{Z}^{(1)}_{\mathrm{em},ij} + 4i\,k\,R^{(6)}_{l,ij}\boldsymbol{S}^{(1)}_{\mathrm{mm},ij},\\
\boldsymbol{Y}^{(7)}_{l,ij} &= R^{(1)}_{l,ij}\boldsymbol{Z}^{(1)*}_{\mathrm{me},ij} + R^{(2)}_{l,ij}\boldsymbol{Z}^{(1)*}_{\mathrm{em},ij} - 4i\,k\,R^{(3)}_{l,ij}\boldsymbol{S}^{(1)*}_{\mathrm{mm},ij} + R^{(4)}_{l,ij}\boldsymbol{Z}^{(1)}_{\mathrm{em},ij} + R^{(5)}_{l,ij}\boldsymbol{Z}^{(1)}_{\mathrm{me},ij} - 4i\,k\,R^{(6)}_{l,ij}\boldsymbol{S}^{(1)}_{\mathrm{ee},ij},\\
\boldsymbol{Y}^{(8)}_{l,ij} &= R^{(1)}_{l,ij}\boldsymbol{Z}^{(1)*}_{\mathrm{mm},ij} - R^{(2)}_{l,ij}\boldsymbol{Z}^{(1)*}_{\mathrm{ee},ij} - 4i\,k\,R^{(3)}_{l,ij}\boldsymbol{S}^{(1)}_{\mathrm{em},ij} + R^{(4)}_{l,ij}\boldsymbol{Z}^{(1)}_{\mathrm{mm},ij} - R^{(5)}_{l,ij}\boldsymbol{Z}^{(1)}_{\mathrm{ee},ij} + 4i\,k\,R^{(6)}_{l,ij}\boldsymbol{S}^{(1)*}_{\mathrm{em},ij},\\
\boldsymbol{Y}^{(9)}_{l,ij} &= i\,R^{(4)}_{l,ij}\big[\boldsymbol{Z}^{(1)}_{\mathrm{ee},ij} - \boldsymbol{Z}^{(1)*}_{\mathrm{mm},ij}\big] + i\,R^{(5)}_{l,ij}\big[\boldsymbol{Z}^{(1)*}_{\mathrm{ee},ij} - \boldsymbol{Z}^{(1)}_{\mathrm{mm},ij}\big] - 4k\,R^{(7)}_{l,ij}\boldsymbol{S}^{(1)*}_{\mathrm{em},ij} - 4k\,R^{(6)}_{l,ij}\boldsymbol{S}^{(1)}_{\mathrm{em},ij},\\
\boldsymbol{Y}^{(10)}_{l,ij} &= R^{(4)}_{l,ij}\big[\boldsymbol{Z}^{(1)}_{\mathrm{me},ij} + \boldsymbol{Z}^{(1)*}_{\mathrm{me},ij}\big] + R^{(5)}_{l,ij}\big[\boldsymbol{Z}^{(1)*}_{\mathrm{em},ij} + \boldsymbol{Z}^{(1)}_{\mathrm{em},ij}\big] + 4i\,k\,R^{(7)}_{l,ij}\boldsymbol{S}^{(1)}_{\mathrm{ee},ij} + 4i\,k\,R^{(6)}_{l,ij}\boldsymbol{S}^{(1)}_{\mathrm{mm},ij},\\
\boldsymbol{Y}^{(11)}_{l,ij} &= R^{(4)}_{l,ij}\big[\boldsymbol{Z}^{(1)}_{\mathrm{em},ij} + \boldsymbol{Z}^{(1)*}_{\mathrm{em},ij}\big] + R^{(5)}_{l,ij}\big[\boldsymbol{Z}^{(1)*}_{\mathrm{me},ij} + \boldsymbol{Z}^{(1)}_{\mathrm{me},ij}\big] - 4i\,k\,R^{(7)}_{l,ij}\boldsymbol{S}^{(1)}_{\mathrm{mm},ij} - 4i\,k\,R^{(6)}_{l,ij}\boldsymbol{S}^{(1)}_{\mathrm{ee},ij}.
\end{aligned} \tag{32}$$

The coefficients Q and R above, dependent on x_{ij}, are all defined in Appendix E in terms of Legendre polynomials. Writing the Q and R coefficients in terms of Legendre polynomials, instead of coefficients $c_{l,m}$, $f_{l,m}$, $g_{l,m}$, and $h_{l,m}$ in Eqs. (8), serves to keep stability in numerical calculation even in large orders l [35]. Equations (31) represent formulations of optical total force on the spherical chiral particle in a discrete spectrum of plane waves. One can further get the expressions for gradient force and scattering force by separating the field-related quantities $\boldsymbol{Z}$ and $\boldsymbol{S}$ included in $\boldsymbol{Y}$ given in Eq. (32). Inserting the pair representation Eqs. (27) into Eqs. (23), one arrives, after some algebra, at a decomposed formulation for the $\boldsymbol{S}$ vectors,

$$\begin{aligned}
\boldsymbol{S}^{(1)\,\mathrm{g}}_{\mathrm{ee},ij} &= -\frac{i/k}{1-x_{ij}}\mathrm{Re}\nabla D^{(1)}_{\mathrm{em},ij}, \quad \boldsymbol{S}^{(1)\,\mathrm{g}}_{\mathrm{mm},ij} = \frac{i/k}{1-x_{ij}}\mathrm{Re}\nabla D^{(1)}_{\mathrm{em},ij},\\
\boldsymbol{S}^{(1)\,\mathrm{g}}_{\mathrm{em},ij} &= \frac{i/k}{2(1-x_{ij})}\,\mathrm{Re}\left[\nabla D^{(1)}_{\mathrm{ee},ij} - \nabla D^{(1)}_{\mathrm{mm},ij}\right],
\end{aligned} \tag{33}$$

and

$$\begin{aligned}
\boldsymbol{S}^{(1)\,\mathrm{s}}_{\mathrm{ee},ij} &= -\frac{i/k^2}{1-x_{ij}}\mathrm{Im}\nabla\times\boldsymbol{G}^{(1)}_{\mathrm{ee},ij} + \boldsymbol{S}^{(1)}_{\mathrm{ee},ij}\delta_{i,j}, \quad \boldsymbol{S}^{(1)\,\mathrm{s}}_{\mathrm{mm},ij} = -\frac{i/k^2}{1-x_{ij}}\mathrm{Im}\nabla\times\boldsymbol{G}^{(1)}_{\mathrm{mm},ij} + \boldsymbol{S}^{(1)}_{\mathrm{mm},ij}\delta_{i,j},\\
\mathrm{Im}\,\boldsymbol{S}^{(1)\,\mathrm{s}}_{\mathrm{em},ij} &= \frac{1/k^2}{2(1-x_{ij})}\mathrm{Im}\big[\nabla\times\boldsymbol{G}^{(1)*}_{\mathrm{me},ij} - \nabla\times\boldsymbol{G}^{(1)}_{\mathrm{em},ij}\big] + \boldsymbol{S}^{(1)}_{\mathrm{em},ij}\delta_{i,j},
\end{aligned} \tag{34}$$

where $\delta_{i,j}$ represents the Kronecker δ. Similarly, the $\boldsymbol{Z}$ vectors are also separated as follows:

$$\boldsymbol{Z}^{(1)\,\mathrm{g}}_{\mathrm{ee},ij} = \tfrac{1}{2}\,\nabla D^{(1)}_{\mathrm{ee},ij}, \qquad \boldsymbol{Z}^{(1)\,\mathrm{g}}_{\mathrm{mm},ij} = \tfrac{1}{2}\,\nabla D^{(1)}_{\mathrm{mm},ij}, \quad \boldsymbol{Z}^{(1)\,\mathrm{g}}_{\mathrm{me},ij} = \tfrac{1}{2}\,\nabla D^{(1)}_{\mathrm{me},ij}, \quad \boldsymbol{Z}^{(1)\,\mathrm{g}}_{\mathrm{em},ij} = \tfrac{1}{2}\,\nabla D^{(1)}_{\mathrm{em},ij}, \tag{35}$$

and

$$\begin{aligned}
\boldsymbol{Z}^{(1)\,\mathrm{s}}_{\mathrm{ee},ij} &= -\tfrac{1}{2}\left[\nabla\times\boldsymbol{S}^{(1)}_{\mathrm{ee},ij} + 2i\,k\,\mathrm{Re}\,\boldsymbol{S}^{(1)}_{\mathrm{em},ij}\right], \quad \boldsymbol{Z}^{(1)\,\mathrm{s}}_{\mathrm{mm},ij} = -\tfrac{1}{2}\left[\nabla\times\boldsymbol{S}^{(1)}_{\mathrm{mm},ij} + 2i\,k\,\mathrm{Re}\,\boldsymbol{S}^{(1)}_{\mathrm{em},ij}\right],\\
\boldsymbol{Z}^{(1)\,\mathrm{s}}_{\mathrm{me},ij} &= -\tfrac{1}{2}\left[\nabla\times\boldsymbol{S}^{(1)}_{\mathrm{me},ij} + i\,k\left(\boldsymbol{S}^{(1)}_{\mathrm{ee},ij} + \boldsymbol{S}^{(1)}_{\mathrm{mm},ij}\right)\right], \quad \boldsymbol{Z}^{(1)\,\mathrm{s}}_{\mathrm{em},ij} = -\tfrac{1}{2}\left[\nabla\times\boldsymbol{S}^{(1)}_{\mathrm{em},ij} - i\,k\left(\boldsymbol{S}^{(1)}_{\mathrm{ee},ij} + \boldsymbol{S}^{(1)}_{\mathrm{mm},ij}\right)\right].
\end{aligned} \tag{36}$$

In Eqs. (33)–(36), terms with the superscript "g" and "s" make contributions to the gradient and scattering forces, respectively. It is noted that in Eqs. (36), each term Re $\boldsymbol{S}^{(1)}_{\mathrm{em},ij}$ in pair representation may no longer be purely solenoidal, but they still contribute solely to the scattering force; see Ref. [35] for a proof.

Equations (31)–(36) constitute the formulations for optical force and its two decomposed parts, gradient and scattering forces, on a chiral sphere immersed in optical field composed of arbitrary number of interferential plane waves. They can actually be applied to calculate optical forces, in particular, two partitioned forces, for arbitrary optical beam, since a discrete spectrum of plane waves can approximately make up arbitrary optical fields.

III. APPLICATION AND EXAMPLE: HIDDEN SYMMETRY AND INVARIANCE IN OPTICAL FORCE

In this section, as an example of application, we calculate the optical forces, both un-decomposed total force and the decomposed gradient and scattering forces, on a spherical chiral particle immersed in TWIF [36,40] composed of three plane waves with the same amplitude and wavelength and their wave vectors forming a regular triangle.

The electric field of the TWIF is described by Eq. (25), with $n_p = 3$ and the complex amplitude vector $\boldsymbol{\mathcal{E}}_i$ of the ith plane wave is given by

$$\boldsymbol{\mathcal{E}}_i = p_i\hat{\boldsymbol{\theta}}_{k_i} + q_i\hat{\boldsymbol{\phi}}_{k_i}, \quad i = 1, 2, 3, \tag{37}$$

where $\hat{\boldsymbol{\theta}}_{k_i}$ and $\hat{\boldsymbol{\phi}}_{k_i}$ represent, respectively, the directions of increasing polar angle and azimuthal angle in spherical coordinate system for the ith wave vector $\boldsymbol{k}_i$. Two complex numbers p_i and q_i form a complex vector (p_i, q_i) known as polarization vector of the ith plane wave. The directions of the wave vectors $\boldsymbol{k}_i$ are characterized by the polar angle θ_{k_i} and azimuthal angle ϕ_{k_i} in the spherical coordinate system,

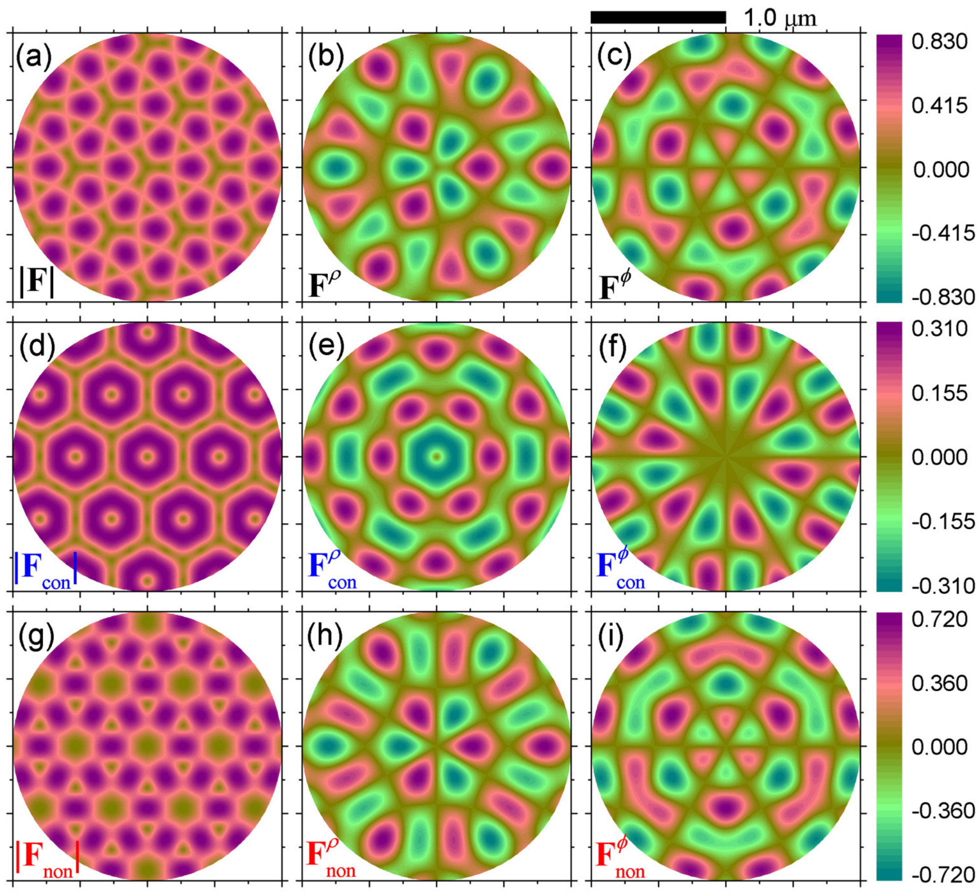

FIG. 1. The spatial profiles of optical forces on a nonchiral polystyrene sphere ($\varepsilon_p = 2.53$, $\mu_p = 1.0$) immersed in the three-wave interference fields on x-o-y plane. The particle radius is $r_p = 0.3\,\mu$m and the polarization vector given in Eq. (39) is $(p, q) = (1, i)/\sqrt{2}$. [(a)–(c)] The magnitude of the undecomposed total optical force $|\boldsymbol{F}|$, its radial component $\boldsymbol{F}^\rho$, and azimuthal component $\boldsymbol{F}^\phi$, respectively. [(d)–(f)] The same as panels (a)–(c), except that the conservative part $\boldsymbol{F}_{\rm con}$ of the optical force $\boldsymbol{F}$ are shown. [(g)–(i)] The same as panels (a)–(c), except that the nonconservative part $\boldsymbol{F}_{\rm non}$ of the optical force $\boldsymbol{F}$ are plotted. The conservative force shows the sixfold even symmetry while the nonconservative force exhibits the sixfold odd symmetry. The symmetry are completely masked in the undecomposed total force that only displays threefold symmetry.

given by

$$(\theta_{k_1}, \phi_{k_1}) = \left(\frac{\pi}{2}, 0\right), \quad (\theta_{k_2}, \phi_{k_2}) = \left(\frac{\pi}{2}, \frac{2\pi}{3}\right),$$
$$(\theta_{k_3}, \phi_{k_3}) = \left(\frac{\pi}{2}, \frac{4\pi}{3}\right). \tag{38}$$

The three plane waves possess the same polarization so that

$$(p_1, q_1) = (p_2, q_2) = (p_3, q_3) = (p, q), \tag{39}$$

which are all normalized to 1, viz. $|p|^2 + |q|^2 = 1$, before the calculation of various optical forces. In the numerical calculation, the light wavelength is set to be $\lambda = 1.064\,\mu$m. The uniform background medium, which does not affect the symmetry and invariance properties, is assumed as water with refractive index $n_b = 1.33$.

Figure 1 shows the spatial profiles of in-plane optical forces for a conventional polystyrene spherical particle with permittivity $\varepsilon_p = 2.53$ and radius $r_p = 0.3\,\mu$m. The particle is immersed in the TWIF composed by three left circularly polarized plane waves, viz. $(p, q) = (1, i)/\sqrt{2}$ in Eq. (39). As demonstrated in Fig. 2 of Ref. [34], the undecomposed total optical force on the particle displays threefold rotational symmetry, a signature of optical fields in the TWIF. This is shown in Figs. 1(a)–1(c) for, respectively, the spatial profiles of the amplitudes of the undecomposed total force $|\boldsymbol{F}|$, its radial part $\boldsymbol{F}^\rho$, and azimuthal part $\boldsymbol{F}^\phi$ in the x-o-y plane. When the optical force is decomposed into the gradient force $\boldsymbol{F}_{\rm con}$ and scattering force $\boldsymbol{F}_{\rm non}$, higher symmetries masked in total force are revealed. This is presented in Figs. 1(d)–1(f), which demonstrate, respectively, the spatial profiles of the magnitude and the radial and azimuthal components of the in-plane gradient force. The sixfold even symmetry manifests itself as $\hat{\mathcal{R}}(\pi/3)\boldsymbol{F}_{\rm con}(\phi) = \boldsymbol{F}_{\rm con}(\phi + \pi/3)$. Here $\hat{\mathcal{R}}(\phi)$ denotes the rotation about z with rotation angle ϕ. The profiles of in-plane scattering force as presented in Figs. 1(g)–1(i), on the other hand, exhibit sixfold odd symmetry, namely, $\hat{\mathcal{R}}(\pi/3)\boldsymbol{F}_{\rm non}(\phi) = -\boldsymbol{F}_{\rm non}(\phi + \pi/3)$. These additional even and odd rotational symmetries are completely obscured in the undecomposed total force; see Figs. 1(a)–1(c). Only when the optical force is decomposed into the gradient and scattering forces can the symmetry make its appearance. The results,

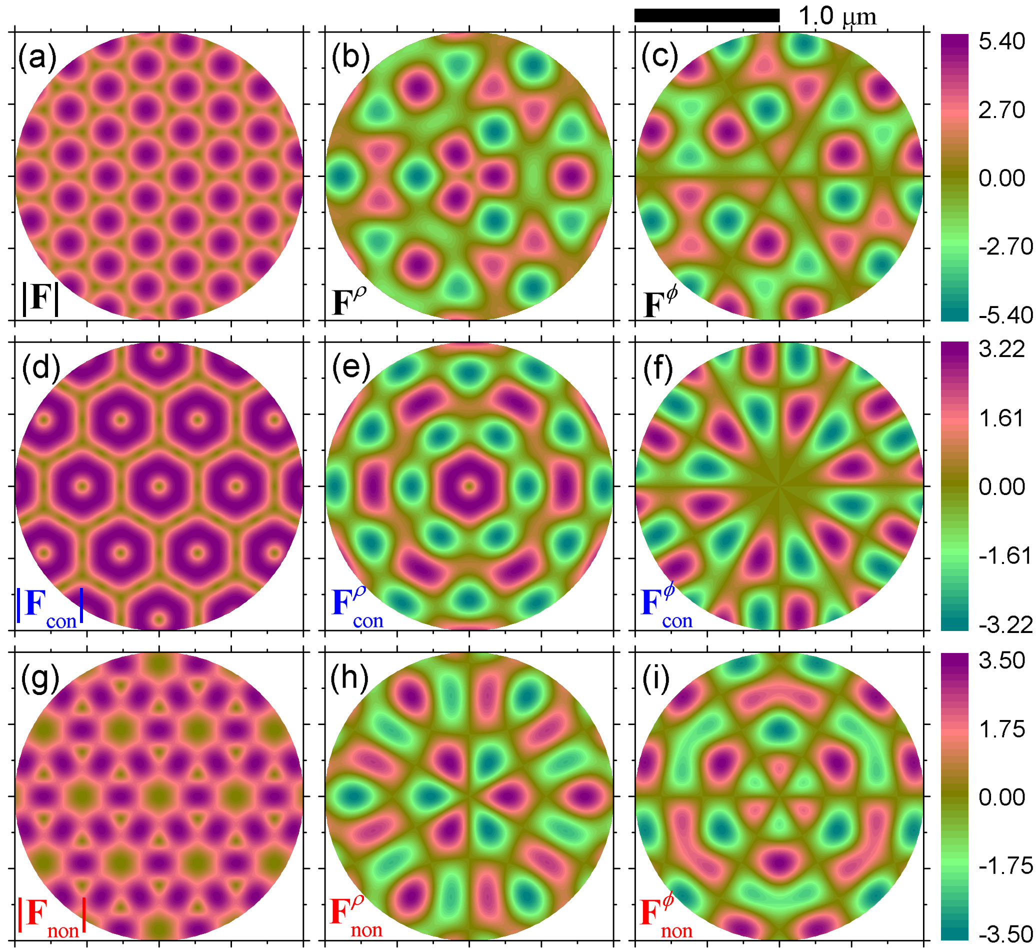

FIG. 2. The same as Fig. 1 except for a chiral particle characterized by a chirality parameter $\kappa = 0.3$ and having the same permittivity and permeability as in Fig. 1.

calculated based on the formulations given in Eqs. (31)–(36), reproduce exactly those in Ref. [34].

Such hidden symmetry survives even when particle is chiral, as shown in Fig. 2, where all the settings are the same as Fig. 1 except $\kappa = 0.3$. In fact, the profiles for decomposed forces $\boldsymbol{F}_{\mathrm{con}}$ in Figs. 2(d)–2(f) and $\boldsymbol{F}_{\mathrm{non}}$ in Figs. 2(g)–2(i) are exactly reproductions of the corresponding profiles in Fig. 1, except for the difference in amplitude. As a result, the spatial profiles for the decomposed gradient and scattering forces are invariant even when the particle carries material chirality. So the hidden symmetry is kept for the chiral case. However, the profiles for the undecomposed total force change radically when particle chirality changes, as can be seen by comparing Figs. 1(a)–1(c) and Figs. 2(a)–2(c). To further corroborate the invariance of the decomposed forces, we show in Fig. 3 the normalized amplitudes of the in-plane total force, the gradient force, and the scattering force along the x axis. The normalization is made by dividing the optical forces on a chiral particle by the corresponding forces acting on a conventional polystyrene sphere with $r_{\mathrm{p}} = 0.3\,\mu$m and located at the same position on the x axis. Figure 3(a) shows the normalized force for a large sphere $r_{\mathrm{p}} = 48.5\,\mu$m with $\kappa = 0.3$, $\varepsilon_{\mathrm{p}} = 2.53$, $\mu_{\mathrm{p}} = 1.0$, and the polarization being $(p, q) = (1, 0.5 + i)$ (before normalization), while Fig. 3(b) displays the results for another case with a higher index sphere, specifically, with $\kappa = 2.0$, $\varepsilon_{\mathrm{p}} = 9.0$, $\mu_{\mathrm{p}} = 3.0$, $r_{\mathrm{p}} = 57.5\,\mu$m, and $(p, q) = (1 - 0.3\,i, -0.5 + i)$ (before normalization). The lines for both the gradient force (dotted blue) and the scattering force (dashed red) stay exactly horizontal along the x axes, indicating the invariance of the spatial profiles of the decomposed forces with respect to particle size, composition, chirality, as well as the polarization of plane waves making up the TWIF. The normalized undecomposed total optical force, however, shows drastic change as the the particle position changes, implying that the invariance is completely ruined for the total force.

IV. SUMMARY

To summarize, after presenting the Cartesian multipole expansion theory up to arbitrary orders of multipoles for computing optical force on a spherical chiral particle located in generic monochromatic optical fields, we develop the rigorous analytical formulations for decomposing the optical force into the gradient and scattering forces, for a spherical chiral particle of arbitrary size and material. A set of analytical expressions are derived that give the optical force and, in particular, its two decomposed constituents, in explicit terms of the impinging electric and magnetic fields for the cases where the incident light is composed of arbitrary numbers of interferential plane waves. Because generic monochromatic optical

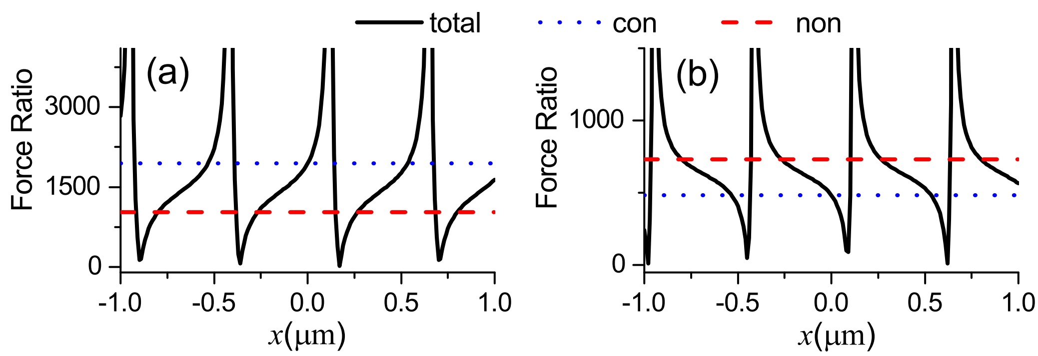

FIG. 3. The magnitudes of the total force $\boldsymbol{F}$ (total, solid black lines), conservative force $\boldsymbol{F}_{\rm con}$ (con, dotted blue lines), and nonconservative force $\boldsymbol{F}_{\rm non}$ (non, dashed red lines) exerting on a spherical chiral particle located on the x axis. The force magnitude is normalized by their corresponding parts in Figs. 1(a), 1(d) and 1(g). (a) A sphere with $\kappa = 0.3$, $\varepsilon_{\rm p} = 2.53$, $\mu_{\rm p} = 1.0$, and $r_{\rm p} = 48.5$ μm. The polarization given in Eq. (39) is set to $(p, q) = (1, 0.5 + i)$ before normalized to 1. (b) A high-index sphere with $\kappa = 2.0$, $\varepsilon_{\rm p} = 9.0$, $\mu_{\rm p} = 3.0$, and $r_{\rm p} = 57.5$ μm. The polarization is defined by $(p, q) = (1 - 0.3\,i, -0.5 + i)$ before normalization. The straight horizontal dotted blue and dashed red lines indicate the invariance of the spatial profiles in both decomposed optical forces with respect to the particle size and material parameters even for chiral cases.

fields can be written as a sum of interferential plane waves, our expressions apply indeed to arbitrary optical beams. As application examples of our formulations, we compute the spatial profiles of the gradient and scattering forces acting on a spherical chiral particle immersed in the TWIF. The profiles reveal the higher degree of symmetry in the decomposed conservative and nonconservative forces than in the undecomposed total optical force, as well as the invariance of the spatial profiles with respect to particle size and material that is completely masked in the total force, as previously reported for conventional particles, even when a particle possesses chirality. We hope the formulations, together with the results concerning the hidden symmetry and invariance of optical force, would cast some light on the in-depth understanding of light-matter interaction, besides opening an avenue for the design of an optical beam to implement more diversified optical micromanipulations.

ACKNOWLEDGMENTS

This work is supported by National Natural Science Foundation of China (Grants No. 11574055 and No. 11804061), National Key R&D Program of China (Grants No. 2018YFA0306201 and No. 2016YFA0301103), Natural Science Foundation of Guangxi Province (No. 2018GXNSFBA281021), Scientific Base and Talent Special Project of Guangxi Province (No. AD19110095), and Open Project of State Key Laboratory of Surface Physics in Fudan University (Grant No. KF2019_11). X Li and Jack Ng are supported by the National Natural Science Foundation of China through Grant No. 11304260.

APPENDIX A: DERIVATION OF Eq. (4)

In free space, any monochromatic incident electric and magnetic fields can be expanded in terms of vector spherical wave functions (VSWFs) $\boldsymbol{M}_{ml}^{(1)}$ and $\boldsymbol{N}_{ml}^{(1)}$

$$\begin{aligned} \boldsymbol{E}_{\rm inc} &= -\sum_{l=1}^{\infty}\sum_{m=-l}^{l} i^{l+1} C_{ml} E_0 \big[\, p_{m,l} \boldsymbol{N}_{ml}^{(1)}(k, \boldsymbol{r}) + q_{m,l} \boldsymbol{M}_{ml}^{(1)}(k, \boldsymbol{r}) \,\big], \\ \boldsymbol{H}_{\rm inc} &= -\frac{1}{Z_0}\sum_{l=1}^{\infty}\sum_{m=-l}^{l} i^{l} C_{ml} E_0 \big[\, q_{m,l} \boldsymbol{N}_{ml}^{(1)}(k, \boldsymbol{r}) + p_{m,l} \boldsymbol{M}_{ml}^{(1)}(k, \boldsymbol{r}) \,\big], \end{aligned} \tag{A1}$$

since both fields are divergence free [45]. Here $Z_0 = \sqrt{\mu_0/\varepsilon_0}$ is the wave impedance in free space, E_0 characterizes the incident field amplitude, and

$$C_{ml} = \left[\frac{(2l+1)}{l(l+1)} \frac{(l-m)!}{(l+m)!} \right]^{1/2}. \tag{A2}$$

So arbitrary monochromatic incident fields are completely characterized by the coefficients $p_{m,l}$ and $q_{m,l}$, which are known as the partial wave expansion coefficients, or beam shape coefficients [33]. The VSWFs $\boldsymbol{M}_{ml}^{(1)}$ and $\boldsymbol{N}_{ml}^{(1)}$ in Eq. (A1) are regular ones, given by (see, e.g., Refs. [42,45,54,55])

$$
\begin{aligned}
\boldsymbol{M}^{(1)}_{ml}(k,\boldsymbol{r}) &= [i\,\pi_{ml}(\cos\theta)\,\boldsymbol{e}_\theta - \tau_{ml}(\cos\theta)\,\boldsymbol{e}_\phi]\frac{\psi_l(kr)}{kr}e^{i\,m\phi},\\
\boldsymbol{N}^{(1)}_{ml}(k,\boldsymbol{r}) &= [\tau_{ml}(\cos\theta)\,\boldsymbol{e}_\theta + i\,\pi_{ml}(\cos\theta)\,\boldsymbol{e}_\phi]\frac{\psi_l'(kr)}{kr}e^{i\,m\phi} + \boldsymbol{e}_r l(l+1)P_l^m(\cos\theta)\frac{\psi_l(kr)}{(kr)^2}e^{i\,m\phi},
\end{aligned}
\tag{A3}
$$

where $\psi_l(x)$ denotes the Riccati Bessel function [42], and $\pi_{ml}(\cos\theta)$ and $\tau_{ml}(\cos\theta)$ are defined by

$$
\pi_{ml}(\cos\theta) = \frac{m}{\sin\theta}P_l^m(\cos\theta), \qquad \tau_{ml}(\cos\theta) = \frac{d}{d\theta}P_l^m(\cos\theta),
\tag{A4}
$$

with $P_l^m(x)$ denoting the associated Legendre function of the first kind [42]. The electromagnetic fields $\boldsymbol{E}_s$ and $\boldsymbol{H}_s$ scattered off the particle are also expanded in terms of VSWFs,

$$
\begin{aligned}
\boldsymbol{E}_s &= \sum_{l=1}^{\infty}\sum_{m=-l}^{l} i^{l+1}C_{ml}E_0\big[\,a_{m,l}\boldsymbol{N}^{(3)}_{ml}(k,\boldsymbol{r}) + b_{m,l}\boldsymbol{M}^{(3)}_{ml}(k,\boldsymbol{r})\,\big],\\
\boldsymbol{H}_s &= \frac{1}{Z_0}\sum_{l=1}^{\infty}\sum_{m=-l}^{l} i^{l}C_{ml}E_0\big[\,b_{m,l}\boldsymbol{N}^{(3)}_{ml}(k,\boldsymbol{r}) + a_{m,l}\boldsymbol{M}^{(3)}_{ml}(k,\boldsymbol{r})\,\big],
\end{aligned}
\tag{A5}
$$

where the outgoing VSWFs $\boldsymbol{M}^{(3)}_{ml}$ and $\boldsymbol{N}^{(3)}_{ml}$, describing the multipole fields [44,45], are given by Eq. (A3) after replacing the Riccati Bessel functions $\psi(x)$ with the Riccati Hankel functions $\xi(x)$ [42]. Then the coefficients $a_{m,l}$ and $b_{m,l}$ for the scattered fields depend on the coefficients $p_{m,l}$ and $q_{m,l}$ for the incident fields through

$$
a_{m,l} = a_l\,p_{m,l} + c_l\,q_{m,l}, \quad b_{m,l} = c_l\,p_{m,l} + b_l\,q_{m,l},
\tag{A6}
$$

for a spherical chiral particle, where the Mie coefficients are given in Ref. [48].

By comparing the electromagnetic fields scattered off the particle written in terms of VSWFs (spherical multipoles) and in terms of Cartesian multipoles [37,42], one derives [37]

$$
\overset{\leftrightarrow}{\mathbb{O}}{}^{(l)}_{\text{elec}} = \gamma_{\text{e}}^{(l)}\sum_{m=0}^{\lfloor\frac{l-1}{2}\rfloor} d_{l,m}\,k^{2m}\,\overset{\leftrightarrow}{\mathbb{N}}{}^{(l,m)}_{\text{elec}}, \quad \overset{\leftrightarrow}{\mathbb{O}}{}^{(l)}_{\text{mag}} = \gamma_{\text{m}}^{(l)}\sum_{m=0}^{\lfloor\frac{l-1}{2}\rfloor} d_{l,m}\,k^{2m}\,\overset{\leftrightarrow}{\mathbb{N}}{}^{(l,m)}_{\text{mag}},
\tag{A7}
$$

for conventional particle with chirality parameter $\kappa = 0$ and thus vanishing c_l in Eq. (A6). Here $d_{l,m}$ is given in Eq. (4), and $\gamma_{\text{e}}^{(l)}$ and $\gamma_{\text{m}}^{(l)}$ are given in Eq. (5), recapitulated here for convenience:

$$
\gamma_{\text{e}}^{(l)} = \frac{\zeta_l\varepsilon_0\,a_l}{k^{2l+1}}, \quad \gamma_{\text{m}}^{(l)} = \frac{\zeta_l\,b_l}{\mu_0\,k^{2l+1}}, \quad \text{with} \quad \zeta_l = \frac{4\pi\,i\,l(2l+1)!!}{(l+1)}.
\tag{A8}
$$

It is thus observed from Eq. (A7) that the electric and magnetic Cartesian multipoles, $\overset{\leftrightarrow}{\mathbb{O}}{}^{(l)}_{\text{elec}}$ and $\overset{\leftrightarrow}{\mathbb{O}}{}^{(l)}_{\text{mag}}$, come, respectively, from the terms proportional to a_l and b_l in the VSWF (spherical multipole) representation; see Eqs. (A5) and (A6). One can therefore map $a_{m,l}$ into $\overset{\leftrightarrow}{\mathbb{O}}{}^{(l)}_{\text{elec}}$ and $b_{m,l}$ into $\overset{\leftrightarrow}{\mathbb{O}}{}^{(l)}_{\text{mag}}$. Taking into account of the electromagnetic duality, one has the mapping $\hat{\mathcal{M}}$

$$
\begin{cases}
\hat{\mathcal{M}}\,[a_{m,l}] = \overset{\leftrightarrow}{\mathbb{O}}{}^{(l)}_{\text{elec}},\\
\hat{\mathcal{M}}\,[b_{m,l}] = \frac{i}{c}\,\overset{\leftrightarrow}{\mathbb{O}}{}^{(l)}_{\text{mag}}.
\end{cases}
\tag{A9}
$$

It follows straightforwardly from Eqs. (A7), (A8), and (A9) that the partial wave expansion coefficients $p_{m,l}$ and $q_{m,l}$ of the incident fields must be transformed as follows:

$$
\begin{aligned}
\hat{\mathcal{M}}\,[p_{m,l}] &= \frac{\zeta_l\varepsilon_0}{k^{2l+1}}\sum_{m=0}^{\lfloor\frac{l-1}{2}\rfloor} d_{l,m}\,k^{2m}\,\overset{\leftrightarrow}{\mathbb{N}}{}^{(l,m)}_{\text{elec}},\\
\hat{\mathcal{M}}\,[q_{m,l}] &= \frac{i\,\zeta_l}{Z_0k^{2l+1}}\sum_{m=0}^{\lfloor\frac{l-1}{2}\rfloor} d_{l,m}\,k^{2m}\,\overset{\leftrightarrow}{\mathbb{N}}{}^{(l,m)}_{\text{mag}},
\end{aligned}
\tag{A10}
$$

so that one has

$$\begin{aligned}\hat{\mathcal{M}}\,[a_{m,l}] &= a_l \hat{\mathcal{M}}\,[p_{m,l}] = \frac{\zeta_l \varepsilon_0 a_l}{k^{2l+1}} \sum_{m=0}^{\lfloor \frac{l-1}{2} \rfloor} d_{l,m}\, k^{2m}\, \overset{\leftrightarrow}{\mathbb{N}}{}^{(l,m)}_{\text{elec}} = \overset{\leftrightarrow}{\mathbb{O}}{}^{(l)}_{\text{elec}},\\ \hat{\mathcal{M}}\,[b_{m,l}] &= b_l \hat{\mathcal{M}}\,[q_{m,l}] = \frac{i\,\zeta_l b_l}{Z_0 k^{2l+1}} \sum_{m=0}^{\lfloor \frac{l-1}{2} \rfloor} d_{l,m}\, k^{2m}\, \overset{\leftrightarrow}{\mathbb{N}}{}^{(l,m)}_{\text{mag}} = \frac{i}{c}\, \overset{\leftrightarrow}{\mathbb{O}}{}^{(l)}_{\text{mag}},\end{aligned} \tag{A11}$$

as given by Eqs. (A7) and (A8).

For the case with $c_l \neq 0$, applying the same mappings $\hat{\mathcal{M}}$ given by Eqs. (A10) to Eqs. (A6), one arrives at

$$\begin{aligned}\hat{\mathcal{M}}\,[a_{m,l}] &= a_l \hat{\mathcal{M}}\,[p_{m,l}] + c_l \hat{\mathcal{M}}\,[q_{m,l}] = \frac{\zeta_l \varepsilon_0 a_l}{k^{2l+1}} \sum_{m=0}^{\lfloor \frac{l-1}{2} \rfloor} d_{l,m}\, k^{2m}\, \overset{\leftrightarrow}{\mathbb{N}}{}^{(l,m)}_{\text{elec}} + \frac{i\,\zeta_l c_l}{Z_0 k^{2l+1}} \sum_{m=0}^{\lfloor \frac{l-1}{2} \rfloor} d_{l,m}\, k^{2m}\, \overset{\leftrightarrow}{\mathbb{N}}{}^{(l,m)}_{\text{mag}},\\ \hat{\mathcal{M}}\,[b_{m,l}] &= b_l \hat{\mathcal{M}}\,[q_{m,l}] + c_l \hat{\mathcal{M}}\,[p_{m,l}] = \frac{i\,\zeta_l b_l}{Z_0 k^{2l+1}} \sum_{m=0}^{\lfloor \frac{l-1}{2} \rfloor} d_{l,m}\, k^{2m}\, \overset{\leftrightarrow}{\mathbb{N}}{}^{(l,m)}_{\text{mag}} + \frac{\zeta_l \varepsilon_0 c_l}{k^{2l+1}} \sum_{m=0}^{\lfloor \frac{l-1}{2} \rfloor} d_{l,m}\, k^{2m}\, \overset{\leftrightarrow}{\mathbb{N}}{}^{(l,m)}_{\text{elec}},\end{aligned} \tag{A12}$$

which are simplified to yield Eqs. (4) and (5) in the main text.

APPENDIX B: SOME MATHEMATICAL IDENTITIES FOR DERIVING Eq. (8)

In deriving Eq. (8) in the main text, we have used the following mathematical identities,

$$\begin{aligned}
[\nabla^{(n)}\boldsymbol{E}^*] \overset{(n)}{\because} \overset{\leftrightarrow}{\mathbb{O}}{}^{(n)}_{\text{elec}} &= \sum_{m=0}^{\lfloor (l-1)/2 \rfloor} c_{l,m}\, k^{4m} \left[\gamma_{\text{e}}^{(l)} \boldsymbol{t}_{\text{ee}}^{(l-2m)} + \gamma_{\text{x}}^{(l)} \boldsymbol{t}_{\text{me}}^{(l-2m)}\right],\\
[\nabla^{(n)}\boldsymbol{B}^*] \overset{(n)}{\because} \overset{\leftrightarrow}{\mathbb{O}}{}^{(n)}_{\text{mag}} &= \sum_{m=0}^{\lfloor (l-1)/2 \rfloor} c_{l,m}\, k^{4m} \left[\gamma_{\text{m}}^{(l)} \boldsymbol{t}_{\text{mm}}^{(l-2m)} - \gamma_{\text{x}}^{(l)} \boldsymbol{t}_{\text{em}}^{(l-2m)}\right],\\
\overset{\leftrightarrow}{\mathbb{O}}{}^{(l)*}_{\text{elec}} \overset{(l)}{\because} \overset{\leftrightarrow}{\mathbb{O}}{}^{(l+1)}_{\text{elec}} &= \sum_{m=0}^{\lfloor \frac{l-1}{2} \rfloor} \Big\{ f_{l,m} k^{4m-2} \big[\eta_{\text{ee}}^{(l)} \boldsymbol{\tau}_{\text{ee}}^{(l-2m)*} + \eta_{\text{ex}}^{(l)} \boldsymbol{\tau}_{\text{em}}^{(l-2m)*} + \eta_{\text{xe}}^{(l)} \boldsymbol{\tau}_{\text{me}}^{(l-2m)*} + \eta_{\text{xx}}^{(l)} \boldsymbol{\tau}_{\text{mm}}^{(l-2m)*}\big]\\
&\quad + g_{l,m} k^{4m} \big[\eta_{\text{ee}}^{(l)} \boldsymbol{\tau}_{\text{ee}}^{(l-2m-1)} + \eta_{\text{ex}}^{(l)} \boldsymbol{\tau}_{\text{me}}^{(l-2m-1)} + \eta_{\text{xe}}^{(l)} \boldsymbol{\tau}_{\text{em}}^{(l-2m-1)} + \eta_{\text{xx}}^{(l)} \boldsymbol{\tau}_{\text{mm}}^{(l-2m-1)}\big]\Big\},\\
\overset{\leftrightarrow}{\mathbb{O}}{}^{(l)*}_{\text{mag}} \overset{(l)}{\because} \overset{\leftrightarrow}{\mathbb{O}}{}^{(l+1)}_{\text{mag}} &= \sum_{m=0}^{\lfloor \frac{l-1}{2} \rfloor} \Big\{ f_{l,m} k^{4m-2} \big[\eta_{\text{mm}}^{(l)} \boldsymbol{\tau}_{\text{mm}}^{(l-2m)*} - \eta_{\text{mx}}^{(l)} \boldsymbol{\tau}_{\text{me}}^{(l-2m)*} - \eta_{\text{xm}}^{(l)} \boldsymbol{\tau}_{\text{em}}^{(l-2m)*} + \eta_{\text{xx}}^{(l)} \boldsymbol{\tau}_{\text{ee}}^{(l-2m)*}\big]\\
&\quad + g_{l,m} k^{4m} \big[\eta_{\text{mm}}^{(l)} \boldsymbol{\tau}_{\text{mm}}^{(l-2m-1)} - \eta_{\text{mx}}^{(l)} \boldsymbol{\tau}_{\text{em}}^{(l-2m-1)} - \eta_{\text{xm}}^{(l)} \boldsymbol{\tau}_{\text{me}}^{(l-2m-1)} + \eta_{\text{xx}}^{(l)} \boldsymbol{\tau}_{\text{ee}}^{(l-2m-1)}\big]\Big\},\\
\Big[\overset{\leftrightarrow}{\mathbb{O}}{}^{(l)}_{\text{elec}} \overset{(l-1)}{\because} \overset{\leftrightarrow}{\mathbb{O}}{}^{(l)*}_{\text{mag}}\Big] \overset{(2)}{\because} \overset{\leftrightarrow}{\boldsymbol{\epsilon}} &= \sum_{m=0}^{\lfloor \frac{l-1}{2} \rfloor} h_{l,m}\, k^{4m} \big[\bar{\eta}_{\text{em}}^{(l)} \boldsymbol{\varsigma}_{\text{exm}}^{(l-2m)} + \bar{\eta}_{\text{xx}}^{(l)} \boldsymbol{\varsigma}_{\text{exm}}^{(l-2m)} + \bar{\eta}_{\text{xe}}^{(l)} \boldsymbol{\varsigma}_{\text{exe}}^{(l-2m)} + \bar{\eta}_{\text{xm}}^{(l)} \boldsymbol{\varsigma}_{\text{mxm}}^{(l-2m)}\big],
\end{aligned} \tag{B1a}$$

where the vectors $\boldsymbol{t}$, $\boldsymbol{\tau}$, and $\boldsymbol{\varsigma}$ are given in Eqs. (11), and the coefficients $c_{l,m}$, $d_{l,m}$, $f_{l,m}$, $g_{l,m}$, and $h_{l,m}$ read

$$\begin{aligned}
d_{l,m} &= \frac{1}{4^m} \frac{l!}{m!} \frac{\Gamma\left(l-m+\frac{1}{2}\right)}{\Gamma\left(l+\frac{1}{2}\right)\Gamma(l-2m)} \frac{1}{l}, \quad \text{with} \quad d_{l,0} = 1,\\
c_{l,m} &= \frac{(l-2m)}{l} (-1)^m d_{l,m} = \frac{l}{(l-2m)} h_{l,m}, \quad \text{with} \quad c_{l,0} = 1,\\
f_{l,m} &= \frac{(l-2m+1)(2l-2m+1)}{(l+1)(2l+1)} (-1)^m d_{l,m}, \quad \text{with} \quad f_{l,0} = 1,\\
g_{l,m} &= \frac{(l-2m)(l-2m-1)}{(l+1)(2l+1)} (-1)^m d_{l,m}, \quad \text{with} \quad g_{l,0} = \frac{l(l-1)}{(l+1)(2l+1)},\\
h_{l,m} &= \frac{(l-2m)^2}{l^2} (-1)^m d_{l,m} = \frac{(l-2m)}{l} c_{l,m} \quad \text{with} \quad h_{l,0} = 1,
\end{aligned} \tag{B2}$$

with $\Gamma(x)$ denoting the Γ function.

APPENDIX C: PROPERTIES FOR FIELD MOMENTS *D*, *S*, and *G*

Here we show some other properties besides those given in Eqs. (18) for field moments D, $\boldsymbol{S}$, and $\boldsymbol{G}$, which may be useful for the derivation of $\boldsymbol{t}$, $\boldsymbol{\tau}$, and $\boldsymbol{\varsigma}$ vectors in the D, $\boldsymbol{S}$, and $\boldsymbol{G}$ representation:

$$\begin{aligned}
\nabla D_{\rm ee}^{(n)} &= 2\omega\,\mathrm{Im}\,\boldsymbol{S}_{\rm em}^{(n)} + 2\,\mathrm{Re}\,\boldsymbol{G}_{\rm ee}^{(n)}, \quad \nabla D_{\rm mm}^{(n)} = -\frac{2\omega}{c^2}\,\mathrm{Im}\,\boldsymbol{S}_{\rm em}^{(n)} + 2\,\mathrm{Re}\,\boldsymbol{G}_{\rm mm}^{(n)},\\
\nabla\times\boldsymbol{S}_{\rm ee}^{(n)} &= -2i\,\mathrm{Im}\big[\boldsymbol{G}_{\rm ee}^{(n)}\big], \quad \nabla\times\boldsymbol{S}_{\rm mm}^{(n)} = -2i\,\mathrm{Im}\big[\boldsymbol{G}_{\rm mm}^{(n)}\big],\\
\nabla\cdot\boldsymbol{S}_{\rm em}^{(n)} &= -\frac{ik}{c}\big[D_{\rm ee}^{(n)} - c^2 D_{\rm mm}^{(n)}\big], \quad \nabla\times\boldsymbol{S}_{\rm em}^{(n)} = \boldsymbol{G}_{\rm me}^{(n)*} - \boldsymbol{G}_{\rm em}^{(n)},\\
\nabla\times\mathrm{Im}\big[\boldsymbol{G}_{\rm ee}^{(n)} + c^2\boldsymbol{G}_{\rm mm}^{(n)}\big] &= -i\big[\boldsymbol{S}_{\rm ee}^{(n+1)} + c^2\boldsymbol{S}_{\rm mm}^{(n+1)}\big] + ik^2\big[\boldsymbol{S}_{\rm ee}^{(n)} + c^2\boldsymbol{S}_{\rm mm}^{(n)}\big]\\
\mathrm{Re}\,\boldsymbol{S}_{\rm ee}^{(n)} &= 0, \quad \mathrm{Re}\,\boldsymbol{S}_{\rm mm}^{(n)} = 0.
\end{aligned} \tag{C1}$$

Actually, the four $\boldsymbol{G}$ vectors can be expressed in terms of others,

$$\begin{aligned}
\boldsymbol{G}_{\rm em}^{(n)} &= -\frac{k}{2c}\left[i\,\boldsymbol{S}_{\rm ee}^{(n)} - i\,c^2\,\boldsymbol{S}_{\rm mm}^{(n)} - \frac{c}{k}\nabla D_{\rm em}^{(n)} + \frac{c}{k}\nabla\times\boldsymbol{S}_{\rm em}^{(n)}\right],\\
\boldsymbol{G}_{\rm me}^{(n)} &= -\frac{k}{2c}\left[i\,\boldsymbol{S}_{\rm ee}^{(n)} - i\,c^2\,\boldsymbol{S}_{\rm mm}^{(n)} - \frac{c}{k}\nabla D_{\rm em}^{(n)*} - \frac{c}{k}\nabla\times\boldsymbol{S}_{\rm em}^{(n)*}\right],\\
\boldsymbol{G}_{\rm ee}^{(n)} &= \frac{1}{2}\nabla D_{\rm ee}^{(n)} - \frac{1}{2}\nabla\times\boldsymbol{S}_{\rm ee}^{(n)} - \omega\,\mathrm{Im}\boldsymbol{S}_{\rm em}^{(n)},\\
\boldsymbol{G}_{\rm mm}^{(n)} &= \frac{1}{2}\nabla D_{\rm mm}^{(n)} - \frac{1}{2}\nabla\times\boldsymbol{S}_{\rm mm}^{(n)} + \frac{\omega}{c^2}\,\mathrm{Im}\boldsymbol{S}_{\rm em}^{(n)}.
\end{aligned} \tag{C2}$$

APPENDIX D: DERIVATION OF EQS. (23)

Here we demonstrate the decomposition of $\boldsymbol{S}_{\rm em}^{(n)}$ as an example; another two vectors $\boldsymbol{S}_{\rm ee}^{(n)}$ and $\boldsymbol{S}_{\rm mm}^{(n)}$ can be separated in the same process. Let us start with the definition of $\boldsymbol{S}_{\rm em}^{(n)}$,

$$\boldsymbol{S}_{\rm em}^{(n)} \equiv [(\nabla^{(n-1)}\boldsymbol{E})\overset{(n-1)}{\vdots}(\nabla^{(n-1)}\boldsymbol{B}^*)]\overset{(2)}{\vdots}\overset{\leftrightarrow}{\boldsymbol{\epsilon}} = \frac{k^{2n-2}}{c}\oint_{4\pi} d\Omega_u \oint_{4\pi} d\Omega_v\,(\boldsymbol{u}\cdot\boldsymbol{v})^{n-1}\,(\boldsymbol{e}_{\boldsymbol{u}}\times\boldsymbol{h}_{\boldsymbol{v}}^*)\,e^{ik(\boldsymbol{u}-\boldsymbol{v})\cdot\boldsymbol{r}}, \tag{D1}$$

which, for $n=1$, delineates the complex Poynting vector $\boldsymbol{S}_{\rm em}^{(1)} = \boldsymbol{E}\times\boldsymbol{B}^*$, the real part of which is associated with the optical momentum density [56] (except for a factor $1/\varepsilon_0$). To write it into an irrotational plus a solenoidal part, a key trick is to multiply the integrand in Eq. (D1) by

$$I = \frac{1}{2}\left[\sum_{m=0}^{\infty}(\boldsymbol{u}\cdot\boldsymbol{v})^m\right](\boldsymbol{u}-\boldsymbol{v})\cdot(\boldsymbol{u}-\boldsymbol{v}), \tag{D2}$$

which is actually equal to unity and thus the multiplication does not change the integral of (D1). Given the mathematical identity

$$[(\boldsymbol{u}-\boldsymbol{v})\cdot(\boldsymbol{u}-\boldsymbol{v})]\boldsymbol{w} = (\boldsymbol{u}-\boldsymbol{v})[\boldsymbol{w}\cdot(\boldsymbol{u}-\boldsymbol{v})] + (\boldsymbol{u}-\boldsymbol{v})\times[\boldsymbol{w}\times(\boldsymbol{u}-\boldsymbol{v})] \tag{D3}$$

for any vector $\boldsymbol{w}$, one gets

$$\begin{aligned}
\boldsymbol{S}_{\rm em}^{(n)} &= \frac{k^{2n-2}}{2c}\oint_{4\pi} d\Omega_u \oint_{4\pi} d\Omega_v \left[\sum_{m=0}^{\infty}(\boldsymbol{u}\cdot\boldsymbol{v})^{m+n-1}\right]\{(\boldsymbol{u}-\boldsymbol{v})[(\boldsymbol{e}_{\boldsymbol{u}}\times\boldsymbol{h}_{\boldsymbol{v}}^*)\cdot(\boldsymbol{u}-\boldsymbol{v})] + (\boldsymbol{u}-\boldsymbol{v})\times[(\boldsymbol{e}_{\boldsymbol{u}}\times\boldsymbol{h}_{\boldsymbol{v}}^*)\times(\boldsymbol{u}-\boldsymbol{v})]\}\,e^{ik(\boldsymbol{u}-\boldsymbol{v})\cdot\boldsymbol{r}}\\
&= \frac{k^{2n-2}}{2c}\oint_{4\pi} d\Omega_u \oint_{4\pi} d\Omega_v \left[\sum_{m=0}^{\infty}(\boldsymbol{u}\cdot\boldsymbol{v})^{m+n-1}\right]\{(\boldsymbol{u}-\boldsymbol{v})[(\boldsymbol{h}_{\boldsymbol{u}}\cdot\boldsymbol{h}_{\boldsymbol{v}}^*) - (\boldsymbol{e}_{\boldsymbol{u}}\cdot\boldsymbol{e}_{\boldsymbol{v}}^*)] - (\boldsymbol{u}-\boldsymbol{v})\times[(\boldsymbol{u}\cdot\boldsymbol{h}_{\boldsymbol{v}}^*)\boldsymbol{e}_{\boldsymbol{u}}\\
&\quad + (\boldsymbol{v}\cdot\boldsymbol{e}_{\boldsymbol{u}})\boldsymbol{h}_{\boldsymbol{v}}^*]\}\,e^{ik(\boldsymbol{u}-\boldsymbol{v})\cdot\boldsymbol{r}},
\end{aligned}$$

which gives rise to

$$\boldsymbol{S}_{\text{em}}^{(n)} = -\frac{i}{2\omega}\,\nabla \sum_{m=0}^{\infty} \frac{1}{k^{2m}}\big[c^2 D_{\text{mm}}^{(n+m)} - D_{\text{ee}}^{(n+m)}\big] - \frac{1}{2k^2}\,\nabla \times \sum_{m=0}^{\infty} \frac{1}{k^{2m}}\big[\boldsymbol{G}_{\text{em}}^{(n+m)} - \boldsymbol{G}_{\text{me}}^{(n+m)*}\big], \tag{D4}$$

where one has used the definitions Eq. (15) and

$$ik \oint_{4\pi} d\Omega_u \oint_{4\pi} d\Omega_v\,[(\boldsymbol{u}-\boldsymbol{v})\,S]\,e^{ik(\boldsymbol{u}-\boldsymbol{v})\cdot\boldsymbol{r}} = \nabla \oint_{4\pi} d\Omega_u \oint_{4\pi} d\Omega_v\,S\,e^{ik(\boldsymbol{u}-\boldsymbol{v})\cdot\boldsymbol{r}},$$
$$ik \oint_{4\pi} d\Omega_u \oint_{4\pi} d\Omega_v\,[(\boldsymbol{u}-\boldsymbol{v})\times\boldsymbol{V}\,]\,e^{ik(\boldsymbol{u}-\boldsymbol{v})\cdot\boldsymbol{r}} = \nabla\times \oint_{4\pi} d\Omega_u \oint_{4\pi} d\Omega_v\,\boldsymbol{V}\,e^{ik(\boldsymbol{u}-\boldsymbol{v})\cdot\boldsymbol{r}},$$

for arbitrary scalar S and vector $\boldsymbol{V}$ independent of $\boldsymbol{r}$.

APPENDIX E: MATHEMATICAL IDENTITIES FOR DERIVING EQS. (31)

To derive Eqs. (31) in the main text, we have used the following mathematical identities,

$$\frac{2\,l\,(2l-1)!!}{(l-1)!}\sum_{m=0}^{\lfloor\frac{l-1}{2}\rfloor} c_{l,m}\,x_{i,j}^{l-2m-1} = Q_{l,\,ij}^{(1)},$$

$$\frac{2\,l\,(2l-1)!!}{(l-1)!}\sum_{m=0}^{\lfloor\frac{l-1}{2}\rfloor} \frac{l-2m-1}{l-2m}\,c_{l,m}\,x_{i,j}^{l-2m-2} = Q_{l,\,ij}^{(2)},$$

$$\frac{8\,(l+1)\,(2l+1)!!}{(l-1)!}\sum_{m=0}^{\lfloor\frac{l-1}{2}\rfloor} f_{l,m}\,x_{i,j}^{l-2m-1} = R_{l,\,ij}^{(1)},$$

$$\frac{8\,(l+1)\,(2l+1)!!}{(l-1)!}\sum_{m=0}^{\lfloor\frac{l-1}{2}\rfloor} \frac{l-2m-1}{l-2m+1}\,f_{l,m}\,x_{i,j}^{l-2m-2} = R_{l,\,ij}^{(2)},$$

$$\frac{2\,(l+1)\,(2l+1)!!}{(l-1)!}\sum_{m=0}^{\lfloor\frac{l-1}{2}\rfloor} \frac{1}{l-2m+1}\,f_{l,m}\,x_{i,j}^{l-2m-1} = R_{l,\,ij}^{(3)},$$

$$\frac{8\,(l+1)\,(2l+1)!!}{(l-1)!}\sum_{m=0}^{\lfloor\frac{l-2}{2}\rfloor} g_{l,m}\,x_{i,j}^{l-2m-2} = R_{l,\,ij}^{(4)},$$

$$\frac{8\,(l+1)\,(2l+1)!!}{(l-1)!}\sum_{m=0}^{\lfloor\frac{l-2}{2}\rfloor} \frac{l-2m-2}{l-2m}\,g_{l,m}\,x_{i,j}^{l-2m-3} = R_{l,\,ij}^{(5)},$$

$$\frac{2\,(l+1)\,(2l+1)!!}{(l-1)!}\sum_{m=0}^{\lfloor\frac{l-2}{2}\rfloor} \frac{1}{l-2m}\,g_{l,m}\,x_{i,j}^{l-2m-2} = R_{l,\,ij}^{(6)},$$

$$\frac{2\,(l+1)\,(2l+1)!!}{(l-1)!}\sum_{m=0}^{\lfloor\frac{l-2}{2}\rfloor} \frac{1}{l-2m}\,g_{l,m}\,x_{i,j}^{l-2m-2} = R_{l,\,ij}^{(6)},$$

$$\frac{8\,l^4\,(2l-1)!!}{(l-1)!}\sum_{m=0}^{\lfloor\frac{l-1}{2}\rfloor} \frac{l-2m-1}{l-2m}\,h_{l,m}\,x_{i,j}^{l-2m-2} = R_{l,\,ij}^{(4)},$$

$$\frac{8\,l^4\,(2l-1)!!}{(l-1)!}\sum_{m=0}^{\lfloor\frac{l-1}{2}\rfloor} \frac{(l-2m-1)(l-2m-2)}{(l-2m)^2}\,h_{l,m}\,x_{i,j}^{l-2m-3} = R_{l,\,ij}^{(5)},$$

$$\frac{8\,l^4\,(2l-1)!!}{(l-1)!}\sum_{m=0}^{\lfloor\frac{l-1}{2}\rfloor} h_{l,m}\,x_{i,j}^{l-2m-1} = 4\,R_{l,\,ij}^{(7)} + R_{l,\,ij}^{(5)},$$

$$\frac{2\,l^4\,(2l-1)!!}{(l-1)!}\sum_{m=0}^{\lfloor\frac{l-1}{2}\rfloor} \frac{(l-2m-1)}{(l-2m)^2}\,h_{l,m}\,x_{i,j}^{l-2m-2} = R_{l,\,ij}^{(6)}, \tag{E1}$$

where the coefficients $c_{l,m}$, $d_{l,m}$, $f_{l,m}$, $g_{l,m}$, and $h_{l,m}$ are defined in Eq. (B2) before and

$$Q_{l,\,ij}^{(1)} = \sum_{m=1}^{l}{}^{(2)} m(2l+1-m)(2l+1-2m)P_{l-m}(x_{ij}),$$

$$Q_{l,\,ij}^{(2)} = \sum_{m=2}^{l}{}^{(2)} m(2l+1-m)(2l+1-2m)P_{l-m}(x_{ij}),$$

$$R_{l,\,ij}^{(1)} = \sum_{m=1}^{l}{}^{(2)} (m+1)(2l+2-m)(2l+1-2m)[2(m+1)l-(m^2-m-4)]P_{l-m}(x_{ij}),$$

$$R_{l,\,ij}^{(2)} = \sum_{m=2}^{l}{}^{(2)} m(m+2)(2l+1-m)(2l+1-2m)(2l+3-m)P_{l-m}(x_{ij}),$$

$$R_{l,\,ij}^{(3)} = \sum_{m=1}^{l}{}^{(2)} (m+1)(2l+2-m)(2l+1-2m)P_{l-m}(x_{ij}),$$

$$R_{l,\,ij}^{(4)} = \sum_{m=2}^{l}{}^{(2)} (2l+1-m)(2l+1-2m)[2m^2l-m(m+1)(m-2)]P_{l-m}(x_{ij}),$$

$$R_{l,\,ij}^{(5)} = \sum_{m=1}^{l}{}^{(2)} (m+1)(m-1)(2l-m)(2l+2-m)(2l+1-2m)P_{l-m}(x_{ij}),$$

$$R_{l,\,ij}^{(6)} = \sum_{m=2}^{l}{}^{(2)} m(2l+1-m)(2l+1-2m)P_{l-m}(x_{ij}),$$

$$R_{l,\,ij}^{(7)} = \sum_{m=1}^{l}{}^{(2)} (2l+1-2m)(2l^2-2(m-1)l+m^2-m)P_{l-m}(x_{ij}). \tag{E2}$$

The summation $\sum_{m=1}^{l}{}^{(2)}$ and $\sum_{m=2}^{l}{}^{(2)}$ above represent the index m odd and even positive integers satisfying $0 < m \leqslant l$, and $P_n(x)$ is the Legendre polynomial.

[1] L. Kelvin, *The Molecular Tactics of a Crystal* (Clarendon Press, Oxford, UK, 1894).
[2] L. A. Nguyen, H. He, and C. Pham-Huy, Int. J. Biomed. Sci. **2**, 85 (2006).
[3] C. M. Dobson, Nature (London) **426**, 884 (2003).
[4] G. Tkachenko and E. Brasselet, Nat. Commun. **5**, 3577 (2014).
[5] S. B. Wang and C. T. Chan, Nat. Commun. **5**, 3307 (2014).
[6] A. Hayata, J. P. B. Muellera, and F. Capasso, Proc. Natl. Acad. Sci. U.S.A. **112**, 13190 (2015).
[7] H. J. Chen, C. H. Liang, S. Y. Liu, and Z. F. Lin, Phys. Rev. A **93**, 053833 (2016).
[8] T. H. Zhang, M. R. C. Mahdy, Y. Liu, J. H. Teng, C. T. Lim, Z. Wang, and C. W. Qiu, ACS Nano **11**, 4292 (2017).
[9] T. Cao and Y. Qiu, Nanoscale **10**, 566 (2018).
[10] M. Li, S. Yan, Y. Zhang, Y. Liang, P. Zhang, and B. Yao, Phys. Rev. A **99**, 033825 (2019).
[11] A. M. Stalcup, Annu. Rev. Anal. Chem. **3**, 341 (2010).
[12] D. G. Grier, Nature (London) **424**, 810 (2003).
[13] K. Dholakia and T. Čižmár, Nat. Photon. **5**, 335 (2011).
[14] L. N. D. Kallepalli, D. Grojo, L. Charmasson, P. Delaporte, O. Uteza, A. Merlen, A. Sangar, and P. Torchio, J. Phys. D: Appl. Phys. **46**, 145102 (2013).
[15] J. Kepler, *De Cometis Libelli Tres* (Augustae Vindelicorum, Augsburg, 1619).
[16] A. Ashkin, Phys. Rev. Lett. **24**, 156 (1970).
[17] A. Ashkin, J. M. Dziedzic, J. E. Bjorkholm, and S. Chu, Opt. Lett. **11**, 288 (1986).
[18] R. W. Bowman and M. J. Padgett, Rep. Prog. Phys. **76**, 026401 (2013).
[19] A. Ashkin, *Optical Trapping and Manipulation of Neutral Particles using Lasers* (World Scientific, Singapore, 2006).
[20] S. Sukhov and A. Dogariu, Rep. Prog. Phys. **80**, 112001 (2017).

[21] C. Maher-McWilliams, P. Douglas, and P. F. Barker, Nat. Photon. **6**, 386 (2012).
[22] J. Baumgartl, M. Mazilu, and K. Dholakia, Nat. Photon. **2**, 675 (2008).
[23] W. L. Lu, H. J. Chen, S. D. Guo, S. Y. Liu, and Z. F. Lin, Opt. Lett. **43**, 2086 (2018).
[24] J. Chen, J. Ng, Z. F. Lin, and C. T. Chan, Nat. Photon. **5**, 531 (2011).
[25] S. Sukhov and A. Dogariu, Phys. Rev. Lett. **107**, 203602 (2011).
[26] A. Novitsky, C. W. Qiu, and H. F. Wang, Phys. Rev. Lett. **107**, 203601 (2011).
[27] A. Dogariu, S. Sukhov, and J. Sáenz, Nat. Photon. **7**, 24 (2013).
[28] O. Brzobohatý, V. Karásek, M. Šiler, L. Chvátal, T. Čižmár, and P. Zemánek, Nat. Photon. **7**, 123 (2013).
[29] A. Ashkin and J. P. Gordon, Opt. Lett. **8**, 511 (1983).
[30] A. Ashkin, Biophys. J. **61**, 569 (1992).
[31] J. J. Du, C. H. Yuen, X. Li, K. Ding, G. Q. Du, Z. F. Lin, C. T. Chan, and J. Ng, Sci. Rep. **7**, 18042 (2017).
[32] H. X. Zheng, X. N. Yu, W. L. Lu, J. Ng, and Z. F. Lin, Comput. Phys. Commun. **237**, 188 (2019).
[33] G. Gouesbet and G. Gréhan, *Generalized Lorenz-Mie Theories*, 2nd ed. (Springer, Berlin, 2017).
[34] Y. K. Jiang, H. Z. Lin, X. Li, J. Chen, J. J. Du, and J. Ng, ACS Photon. **6**, 2749 (2019).
[35] X. N. Yu, Y. K. Jiang, H. J. Chen, S. Y. Liu, and Z. F. Lin, Phys. Rev. A **100**, 033821 (2019).
[36] G. J. Ha, H. X. Zheng, X. N. Yu, and Z. F. Lin, Phys. Rev. A **100**, 033817 (2019).
[37] Y. K. Jiang, H. J. Chen, J. Chen, J. Ng, and Z. F. Lin, arXiv:1511.08546.
[38] Y. K. Jiang, J. Chen, J. Ng, and Z. F. Lin, arXiv:1604.05138.
[39] G. J. Ha, H. X. Zheng, X. N. Yu, and Z. F. Lin, J. Opt. Soc. Am. B **37**, 67 (2020).
[40] T. V. Raziman and O. J. F. Martin, Phys. Rev. A **98**, 023420 (2018).
[41] H. J. Chen, S. Y. Liu, J. Zi, and Z. F. Lin, ACS Nano **9**, 1926 (2015).
[42] C. F. Bohren and D. R. Huffman, *Absorption and Scattering of Light by Small Particles* (John Wiley, New York, 1998).
[43] M. I. Mishchenko, N. T. Zakharov, N. G. Khlebtsov, T. Wriedt, and G. Videen, J. Quant. Spectrosc. Radiat. Transfer **146**, 349 (2014).
[44] M. E. Rose, *Multipole Fields* (John Wiley, New York, 1955).
[45] J. A. Stratton, *Electromagnetic Theory* (McGraw-Hill, New York, 1941).
[46] B. L. Silver, *Irreducible Tensor Methods* (Academic Press, New York, 1976).
[47] J. Applequist, J. Phys. A **22**, 4303 (1989).
[48] H. J. Chen, N. Wang, W. L. Lu, S. Y. Liu, and Z. F. Lin, Phys. Rev. A **90**, 043850 (2014).
[49] G. Gouesbet and J. A. Lock, J. Quant. Spectrosc. Radiat. Transfer **162**, 18 (2015).
[50] P. C. Clemmow, *The Plane Wave Spectrum Representation of Electromagnetic Fields* (Pergamon Press, Oxford, UK, 1966).
[51] L. Mandel and E. Wolf, *Optical Coherence and Quantum Optics* (Cambridge University Press, Cambridge, UK, 1995).
[52] J. W. Goodman, *Introduction to Fourier Optics* (Roberts and Co., Englewood, Colorado, 2005).
[53] S. Colak, C. Yeh, and L. W. Casperson, Appl. Opt. **18**, 294 (1979).
[54] Y. L. Xu, Appl. Opt. **34**, 4573 (1995).
[55] J. Ng, Z. F. Lin, C. T. Chan, and P. Sheng, Phys. Rev. B **72**, 085130 (2005).
[56] J. D. Jackson, *Classical Electrodynamics* (John Wiley and Sons, New York, 1999).